Scientific Reports

https://doi.org/10.1038/s41598-026-42977-z

Article in Press

Animal-origin-free method for generating blood vessel organoids

Received: 26 November 2025

Accepted: 28 February 2026

Published online: 05 March 2026

Cite this article as: Hoffmann A., Schorn D., Thönig J. *et al.* Animal-origin-free method for generating blood vessel organoids. *Sci Rep* (2026). https://doi.org/10.1038/s41598-026-42977-z

Alexander Hoffmann, David Schorn, Jakob Thönig, Yu-Hsiang Teng, Jean-François Bisson & Teodor E. Yordanov

Animal-Origin-Free Method for Generating Blood Vessel Organoids

Alexander Hoffmann[1,2], David Schorn[1], Jakob Thönig[1], Yu-Hsiang Teng[1], Jean-François Bisson[3], Teodor E. Yordanov[1*]

[1] Angios FlexCo, Innsbruck, Austria
[2] Department of Internal Medicine II, Medical University Innsbruck, Austria
[3] ETAP-Lab, Department of Dermatology, Vandœuvre-lès-Nancy, France

***Correspondence:** Teodor E. Yordanov
Angios FlexCo
Exlgasse 24, 6020 Innsbruck, Austria
Email: teodor.yordanov@angios-bio.com

Abstract

Background: Blood vessel organoids (BVOs) represent a promising tool for modeling vascular diseases, drug screening, and regenerative therapies. However, current protocols for BVO generation are complex, labor-intensive, and reliant on animal-derived extracellular matrices (ECM) such as Matrigel, limiting reproducibility, scalability, and clinical applicability.

Methods: We developed a simplified, animal-origin-free protocol for BVO generation that addresses current limitations and enables high-throughput automated workflows. The method employs ultra-low attachment 96-well U-bottom plates for standardized aggregation and differentiation of human induced pluripotent stem cells (hiPSCs) in a human derived collagen-based extracellular matrix. Unlike conventional protocols where aggregates are embedded in a two-layer ECM, our approach utilizes a single-layer, which we termed “sitting drop”. This innovative approach requires considerably fewer materials and handling steps and is compatible with high-throughput automated machines.

Results: BVO generation utilizing the here described optimized protocol resulted in the formation of BVOs with reproducible morphology and cellular composition. Flow cytometry confirmed the presence of $CD31^+$ endothelial cells and $PDGFR\beta^+$ pericytes in BVOs, generated in sitting drops in ultra-low adhesive U-bottom shaped 96 well plates, with cell population percentages comparable to those observed in traditional two-layer BVO cultures. *In vivo* transplantation of mature BVOs in a mouse full-thickness skin wound model demonstrated integration of BVO derived cells into host vessels, highlighting their potential in cell-based therapies.

Conclusion: Our study presents a robust and animal-origin-free method for BVO generation based on single-layer “sitting drop” cultures. This protocol maintains cellular integrity while enhancing reproducibility and automation-readiness, paving the way for high-throughput screening and clinical translation of vascular organoid technology.

Keywords

Blood Vessel Organoids (BVO), Extracellular Matrix (ECM), Collagen, High-throughput, Organoids, Bioengineering

Highlights

- Entire blood vessel organoid (BVO) workflow performed in a single ultra-low attachment U-bottom shaped 96 well plate
- Fully animal-origin-free: no Matrigel or Geltrex required throughout the protocol
- Robust generation of BVOs using human collagen-based ECM
- High-throughput compatible and automation-ready “sitting drop” culture system
- Integration of BVO-derived cells into host vessels *in vivo*

1. Introduction:

Organoids are three-dimensional *in vitro* models of organs derived from stem cells, including those representing the small intestine (1), liver (2), lung (3), pancreas (4), brain (5), and blood vessels (6), among others. These models hold immense potential for both basic and translational research, enabling high-throughput drug screening, reducing reliance on animal experiments, and paving the way for innovative cell-based therapies and personalized medicine. In particular, Blood Vessel Organoids (BVOs) have emerged as a promising tool for studying vascular diseases such as diabetic vasculopathy (7) and atherosclerosis (8).

Despite their potential, current protocols for generating BVOs face key limitations. Most approaches are based on the protocol by Wimmer et al. (6), which involves the use of animal-derived extracellular matrices such as Matrigel. These matrices are not only expensive and non-compliant with good manufacturing practice (GMP) but also exhibit considerable batch-to-batch variability, significantly compromising reproducibility (9, 10). In addition, the conventional two-layer embedding technique requires manual excising, transferring organoids between plates, which makes the workflow labor-intensive, prone to errors and is poorly suited for automation.

To overcome these limitations, we developed a simplified and animal-origin-free protocol for BVO generation that is compatible with GMP. Our method enabled aggregate formation, differentiation and organoid formation in a single plate using standardized ultra-low attachment 96-well U-bottom plates (ULU-96) and a human-collagen-based extracellular matrix (HC-ECM). Instead of the conventional two-layer embedding method, we introduced a one-step extracellular matrix (ECM) embedding approach that simplifies handling and enhances high-throughput compatibility, which we refer to as the “sitting drop” method.

This work establishes a robust platform for reproducible, animal-origin-free BVO production, paving the way for translational applications in regenerative medicine and disease modeling.

2. Methods:

2.1. Cell culture

Human induced pluripotent stem cells (hiPSC) were purchased from Pluristyx (201 Elliott Ave W, Seattle, WA 98119, USA). Cells were cultured

on Nunc™ Cell-Culture Treated Multidishes 6 Well-plate (ThermoFisherScientific, 150675) precoated with 2 mL DPBS, calcium, magnesium (DPBS +/+) (Gibco, 14040117) and 2.5 µg/mL Biolaminin 521 LN (Biolamina, LN521-05). Plates were incubated in an MCO-230AICUV IncuSafe CO2 Incubator (PHCEurope). Animal origin free culture media was prepared using 47.5 mL TeSR™-AOF Basal medium (STEMCELL, 100-0402) with 2.5 mL TeSR™-AOF 20X Supplement (STEMCELL, 100-0403) and 100 µL Antibiotic Normocin (InvivoGen, NOL-44-09) and was used for up to 2 weeks stored at 4°C. For passaging, 70-80% confluent cells were washed with DPBS, no calcium, no magnesium (DPBS -/-) (Gibco, 14190144) before cell dissociation using ReLeSR (Stemcell, 100-0483) incubated for 1 minute at 37°C. ReLeSR was aspirated, and the plate was incubated for 5 minutes at 37°C with no medium. Cells were resuspended using 1 mL of culture medium and seeded on precoated plates with a minimum dilution of 1:10.

Used plates that are not mentioned in the protocol:

- AggreWell™800, 24 well plate (STEMCELL, Cat. No,: 34815)
- SUN BioScience's, 24 well plate (inSpohero, Cat. No.: GRI3D-24P-C-4-800)
- U-Bottom delta Nunclon ™ Delta Surface 96 well plate (Thermos Scientific, Cat. No.: 163320)
- Flat Bottom Ultra-Low Attachment Surface Costar® 96 well plate (Corning, Cat. No.: 3474)
- Flat Bottom 96 Well Cell Culture Plate, Cellstar (Greiner, Cat.: 655 180)

2.2. Protocol for Blood Vessel Organoid (BVO) Formation and Maturation in Single Layer Sitting Drops in 96 Well Plates:

Day 0: Aggregation Formation

1. Prepare Aggregation Formation Medium

- Mix STEMdiff™ BVO Aggregation Basal Medium (STEMCELL, Cat. No.: 100-0652) with STEMdiff™ BVO Aggregation Supplement (STEMCELL, Cat. No.: 100-0653) in a 4:1 ratio (medium: supplement) at room temperature (RT).
- After mixing at RT (21-24°C), warm the Aggregation Formation Medium to 37 °C.

2. Cell collection and counting

- Dilute 0.5 M EDTA (Invitrogen UltraPure™ 0.5 M EDTA, pH 8.0) to 0.5 mM in DPBS (50 µL EDTA + 50 mL DPBS/PBS without Mg^{2+} and Ca^{2+}) and warm it in the water bath to 37 °C.
- Thaw Accutase (StemPro® Accutase® Cell Dissociation Reagent, Cat. No.: A1110501).
- Aspirate medium from the cells and add 0.6 mL of warm 0.5 mM EDTA in DPBS.
- Incubate at 37 °C and 5% CO_2 for 5 minutes.

- Carefully remove the plate from the incubator, ensuring not to shake.
- Aspirate EDTA solution from the cells without removing the cells.
- Add 0.6 mL of RT Accutase.
- Incubate at 37 °C and 5% CO_2 for 5 minutes.
- Check whether cell detachment is successful by gently tapping the plate.
- Once cells are detached, add 2 × 0.7 mL of Aggregate Formation Medium, collect the cells, and transfer the cell suspension to a sterile 15 mL conical tube.
- Rinse the well with 1 mL of Aggregate Formation Medium and add it to the conical tube.
- Use a P1000 tip to pipette up and down to ensure a homogeneous cell distribution before counting.
- Count the cells using trypan blue and a Countess system (Countess II, Thermo Fisher, Ref: AMQAX1000R), a hemocytometer or a comparable system.
- Calculate the volume of cell suspension required to seed 1000 cells per well and transfer it to a new 15 mL conical tube.

3. Centrifuge and resuspend cells

- Centrifuge the cells at 250-300 × g for 3-5 minutes.
- Add ROCK inhibitor (Y-27632) (Miltenyi, Cat. No.: 130-104-169) to the Aggregation Formation Medium to achieve a final concentration of 50 µM.
- Warm medium to 37 °C before use.
- Remove the supernatant from the cell pellet.
- Resuspend the cell pellet in Aggregation Seeding Medium (with ROCK inhibitor Y-27632) to a concentration of 1000 cells per 50 µL.

4. Seed aggregates

- Add 50 µL of the cell suspension to each well of a 96-well U-bottom ultra-low attachment plate (ULU-96) (e.g., faCelliate BIOFLOAT, Cat. No.: F202003).
- Place the plate in a humidified incubator at 37°C, 5% CO_2.

Day 1: One day after aggregation

1. Microscopic observation

- Examine each well under a microscope to confirm a single, round aggregate with smooth edges. Target diameter is ~200 µm; if aggregates are ~240 µm, proceed directly to Day 2.
- If the aggregates do not have the optimal size, adjust the seeding density on Day 0.

Day 2: Mesoderm induction

1. Microscopic observation

- Aggregates should remain round with smooth edges and grow to a diameter of approximately 240 µm.

2. Prepare Mesoderm Induction Medium (8 mL total is sufficient for 96 wells)

- Thaw supplements to RT (21-24 °C).
- STEMdiff™ BVO Induction Basal Medium (STEMCELL, Cat. No.: 100-0654): 7.760 mL
- STEMdiff™ BVO Induction Supplement (STEMCELL, Cat. No.: 100-0655): 80 µL
- STEMdiff™ BVO Mesodermal Induction Supplement (STEMCELL, Cat. No.: 100-0656): 160 µL
- After mixing at RT, warm the Mesoderm Induction Medium to 37 °C.

3. Medium exchange

- Carefully aspirate all Aggregation Formation Medium from each well and replace with 70 µL of freshly prepared Mesoderm Induction Medium.
- Immediately return the plate to the incubator (37 °C, 5% CO_2).

Day 5: Vascular induction

1. Prepare Vascular Induction Medium (8 mL total is sufficient for 96 wells)

- Thaw supplements to RT (21-24 °C).
- STEMdiff™ BVO Induction Basal Medium (STEMCELL, Cat. No.: 100-0654): 7.760 mL
- STEMdiff™ BVO Induction Supplement (STEMCELL, Cat. No.: 100-0655): 80 µL
- STEMdiff™ BVO Vascular Induction Supplement (STEMCELL, Cat. No.: 100-0657): 160 µL
- After mixing at RT, warm the Vascular Induction Medium to 37 °C.

2. Medium exchange

- Carefully aspirate all Mesoderm Induction Medium from each well and replace with 70 µL of freshly prepared Vascular Induction Medium.
- Immediately return the plate to the incubator (37 °C, 5% CO_2).

Day 7: Embedding and blood vessel network formation

1. Thaw reagents

- Thaw STEMdiff™ Blood Vessel Organoid Maturation Medium (STEMCELL, Cat. No.: 100-0658) at RT (21-24 °C).

2. Microscopic observation

- Aggregates should appear round with flaky or rough edges and grow to a diameter of approximately 470 µm.

3. Prepare nutrient mix on ice

- The calculations below are given per 1 mL (nutrient mix plus collagen mix). However, prepare at least 5 mL total, as smaller volumes affect polymerization.
- Prepare the nutrient mix as follows per mL (adjust to needed volume):
  - Hams F12 Nutrient Mix (Gibco, Cat. No.: 11765-054): 159 µL
  - 5× DMEM/High Glucose (Cytiva, Cat. No.: SH30003.03): 125.2 µL
  - Sterile filtered water: 12.2 µL
  - GlutaMAX (Gibco, Cat. No.: 13462629): 6.4 µL
  - HEPES (Gibco, Cat. No.: 15630080): 12.6 µL
  - Sodium Bicarbonate (Gibco, Cat. No.: 25080-094): 9.8 µL

4. Prepare desired extracellular matrix (ECM):

- **Matrigel/Geltrex-bovine collagen mix:**
  - Use 750 µL collagen mix (PureCol, 3.2 mg/mL, Advanced BioMatrix, Cat. No.: m5005-100ML) + 250 µL Geltrex (Gibco, Cat. No.: A14133-02) or 250 µL Matrigel (Corning, Cat. No.: 356231).
- **Bovine collagen (PureCol) (2.15 mg/mL):**
  - Nutrient mix: 325.2 µL
  - Collagen (PureCol, 3.2 mg/mL, Advanced BioMatrix, Cat. No.: m5005-100ML): 666.6 µL
  - Sodium hydroxide (Sigma, Cat. No.: S2770-100ML): 8.34 µL
- **Human collagen (2mg/mL):**
  - Nutrient mix: 325.2 µL
  - Collagen (3mg/mL) (CellAdhere™ Type I Collagen, Human, STEMCELL, Cat. No.: 07005) 650.4µL

- **NOTE:** The pH of the gel should be between 7.4 and 7.6.
- **NOTE:** Collagen concentration in Geltrex varies (2-5 mg/mL) according to the provider (Gibco) and Matrigel 2-6 mg/mL (Corning) respectively
- **NOTE:** For human collagen we found that collagen concentrations in the range of 1-5 mg/mL provided consistent polymerization and supported stable organoid morphology (see Supp. Fig. 3 A-D).
- Keep the extracellular matrix on ice to prevent polymerization.

5. Embed aggregates

- Completely remove the Vascular Induction Medium without disturbing the aggregates.
- Add 35 µL of extracellular matrix (ECM) to the aggregates in the same ULU-96 plate (20-75 µL of ECM provides stable organoid formation, see Suppl. Fig. 1 H; Suppl. Fig. 2 A-F). The resulting culture of aggregate in ECM is termed “sitting drop”.
- For the sitting drops just let the appropriate amount of ECM drop on the media-free aggregate.

- The aggregate should be positioned in the center of the drop (not at the edges when viewed from above), and the drop should sit in the center of the well (not on the walls).
- Aggregates can be embedded in a collagen I-Matrigel (or Geltrex) mix (3:1) in collagen alone (e.g. PureCol) or in recombinant human collagen I.
- Incubate at 37 °C for at least 2 hours to allow for polymerization.

6. Add Maturation Medium

- After polymerization, add 100-150 µL of warm (37°C) STEMdiff™ BVO Maturation Medium (STEMCELL, Cat. No.: 100-0658) Maturation Medium without disturbing the sitting drops.
- Return the plate to the incubator (37 °C, 5% CO_2) immediately.

Day 8 (embedding day 1):

- Aggregates begin to differentiate into vascular networks. Examine the vascular networks under a microscope and look for radial sprouting.

Day 12 (embedding day 5)

1. Microscopic examination

- Observe the vascular networks / early BVOs under the microscope.
- Note that the gel may appear reduced in volume and partially pulled toward the BVOs. Some BVOs may begin to float in the medium.

2. Medium exchange

- Carefully aspirate the old Maturation Medium from each well, avoiding disruption to the BVOs or gel.
- Add 100-150 µL of fresh, pre-warmed (37°C) STEMdiff™ BVO Maturation Medium (STEMCELL, Cat. No.: 100-0658) Maturation Medium to each well.
- Immediately return the plate to a humidified incubator set at 37°C with 5% CO_2 to ensure optimal growth conditions.

Day 16-23: mature BVOs

1. Microscopic examination

- BVOs should appear rounded, with residual gel at the edges or floating in the medium and are ready to use.

2. Extended culture

- From day 16 onward, change the medium every 2-3 days. During this period, BVOs progressively remodel and consume the surrounding extracellular matrix. For the purposes of this protocol, BVOs are considered *spherical* once they form a stable, self-supporting, rounded

structure that is no longer embedded within the matrix and is readily recognizable as a free-floating sphere by visual inspection. By day 23, BVOs are typically free of extracellular matrix.

2.3. Flow Cytometry:

All data were acquired using a CytoFLEX S flow cytometer (Beckman Coulter) or a NAVIOS flow cytometer (Beckman Coulter) and analyzed with FlowJo software (version 10.10.0, Becton Dickinson). Briefly, three blood BVOs per sample were washed once with RPMI-1640 medium (Gibco, Cat. No.: 11875-093) and digested for approximately 40 minutes at 37°C using the Multi Tissue Dissociation Kit (Miltenyi Biotec, Cat. No.: 130-110-201). The digestion process was stopped by adding cold (4°C) RPMI-1640 supplemented with 10% fetal calf serum (FCS, Fisher Scientific, Cat. No.: 11573397). The cells were then centrifuged at 300 x g for 3 minutes, followed by a single wash with FACS buffer (composed of 1:20 BSA dilution using MACS® BSA Stock Solution, Miltenyi Biotec, Cat. No.: 130-091-376, in autoMACS® Rinsing Solution, Miltenyi Biotec, Cat. No.: 130-091-222). Subsequently, the cells were stained with the following antibodies: Anti-human CD31 (PE, REAfinity™, Clone: REA730, 1:100 dilution, Miltenyi Biotec, Cat. No.: 130-110-669, Lot: 5241009173); Anti-human CD140b (PDGFRβ) (REAfinity™, Clone: REA363, 1:100 dilution, Miltenyi Biotec, Cat. No.: 130-129-294, Lot: 5230704827); Anti-human TRA-1-60 (PE, REAfinity™, Clone: REA157, 1:100 dilution, Milteny Biotec, Cat. No.: 130-122-921, Lot: 5230401683; Anti-human SSEA-4 (APC, REAfinity™, Clone: REA101, 1:100 dilution, Milteny Biotec, Cat. No.: 130-123-815, Lot: 5230502976); Viability dye (eFluor™ 450, 1:1000 dilution, Invitrogen, Cat. No.: 65-0863-14, Lot: 2804457). Staining was performed for 30-60 minutes at RT in the dark. After staining, the cells were washed three times with FACS buffer and resuspended in 300-500 µL of FACS buffer for flow cytometric analysis (Gating strategy see Suppl. Fig. 6).

2.4. Immunofluorescence Staining

Blood vessel organoids were transferred to 2 mL Eppendorf tubes using a cut 1 mL pipette tip with an inner diameter of approximately 1.5-2.0 mm (or a commercially available wide bore 1000 tip; eg. Cat. No.: AXYT1005WBCRS/Corning). After settling, organoids were washed twice with D-PBS (Gibco, Cat. No.: 14190-094) and fixed in 2 mL of 4% paraformaldehyde solution (Fisher Scientific, Cat. No.: 28908) for 60 minutes at RT (21-24°C) on a rocking platform. Fixed organoids were washed twice with D-PBS and stored in D-PBS at 2-8°C for up to one month. For blocking, organoids were incubated with 1 mL of blocking buffer [1% BSA (Roche, Cat. No.: 10735078001), 3% donkey serum (Biowest, Cat. No.: S2170-100), 0.5% Tween-20 (Sigma, Cat. No.: P1379-25 mL), 0.5% Triton X-100 (Sigma, Cat. No.: X-100-100 mL), 0.01% sodium deoxycholate (Sigma, Cat. No.: D6750-10G, from 1% wt/vol stock solution), and 94.99% D-PBS] at RT for 3 hours on a rocking platform.

Primary antibodies, including mouse anti-human CD31 (Agilent, Cat. No.: M0823, Lot: 41355845, Clone: JC70A, 1:100) and rabbit anti-human PDGFRβ (Cell Signaling, Cat. No.: 3169S, Lot: 15, Clone: 28E1, 1:100),

were diluted in blocking buffer. A total of 100 µL of the primary antibody mix was added to the organoids, and the samples were incubated at 4°C overnight on a rocking platform. Following incubation, organoids were washed three times with wash buffer (0.05% Tween-20 in D-PBS), with a 30-minute rocking platform incubation during the third wash.
Secondary antibodies, including Alexa Fluor™ 546 donkey anti-mouse IgG (H+L) (Invitrogen, Cat. No.: A10036, Lot: 2306765, 1:250) and Alexa Fluor™ 647 donkey anti-rabbit IgG (H+L) (Invitrogen, Cat. No.: A31573, Lot: 2752586, 1:250), were diluted in blocking buffer. A total of 250 µL of the secondary antibody mix was added to the organoids, followed by a 3-hour incubation at RT in the dark on a rocking platform. Organoids were washed twice with wash buffer, leaving the second wash for 30 minutes in the dark on a rocking platform.
For clearing, organoids were incubated with 200 µL RapiClear 1.49 (SUNJin Lab, Cat. No.: RC149002) overnight. After clearing, organoids were transferred onto a coverslip with a 1 mm iSpacer (SUNJin Lab, Cat. No.: IS012), and residual RapiClear was carefully removed. For mounting, 300-400 µL RapiClear was applied before placing a coverslip on top. Coverslips were sealed with clear nail polish and stored at 4 °C overnight.

2.4.1. Image acquisition

Image acquisition was performed using a confocal microscope (ZEISS Cell Observer SD), equipped with Neofluar 10x NA 0.3 Objective and Zen 2.6 software (ZEISS, blue edition, Version 2.6.76.00000). Image processing was carried out with the open-source software ImageJ2 (Version 2.16.0/1.54p).

2.4.2. Vascular organoid staining quantification

Endothelial and pericyte signal intensity within organoids were quantified using a custom endothelial-pericyte line intensity analysis, developed in Fiji (ImageJ) macro language. Briefly, organoid images were acquired as 3D single plane confocal images and stacked with ImageJ maximum intensity stacking function. Two channels were analysed: CD31 (endothelial marker) and PDGFRB (pericyte marker). Organoids were analyzed either in full or in part, depending on image coverage. In all cases, a 10-pixel-wide line region of interest (ROI) was consistently placed through the organoid and terminated at the organoid edge. The macro then extracted intensity profiles along this line and performed channel-specific background subtraction and normalization using the equation:

$$I_{norm}(x) = \frac{I(x) - I_{bg}}{I_{signal} - I_{bg}}$$ where I_x means the given signal, I_{bg} represents the mean background intensity, I_{signal} is defined using statistical thresholding (the mean plus two standard deviations of the channel intensity) and $I_{norm}(x)$ is the normalized value. Negative normalized values were clipped to zero. The normalized values in lines were then visualized in Graphpad Prism.

2.5. Mouse Experiments

All animal experiments were carried out in accordance with the guidelines of the European Communities Council Directive of 22 September 2010 on the approximation of laws, regulations, and administrative provisions of the Member States regarding the protection of animals used for scientific purposes, and in compliance with the ARRIVE guidelines. The objective of this single-arm feasibility experiment was to evaluate whether implanted blood vessel organoids (BVOs) could be detected within a full-thickness skin wound environment in NOD SCID gamma mice. The experimental unit was the individual animal. Five 8-week-old male NOD SCID gamma mice (NSG®: NOD.Cg-PrkdcSCID Il2rgtm1Wjl/SzJ; Charles River Laboratories, l'Arbresle, France) were included in the study. No randomization was performed, as this was a single-arm feasibility experiment, and blinding was not performed. Animals were individually housed at ETAP-Lab (Nancy, France) under conventional husbandry conditions in an inverted 12-hour light/12-hour dark cycle (lights off from 08:00 to 20:00), at 24 ± 2°C and 50 ± 20% relative humidity, with food and water ad libitum. Environmental enrichment consisted of a sizzle nest, square pieces of paper, and a dome. On Day 0, mice were placed under gas anesthesia with isoflurane (Iso-Vet, Piramal Critical Care) in a 70%/30% air/O_2 mixture at 2.5% for induction and 1.5% for maintenance, and body temperature was maintained at 35–37°C using a temperature-maintaining heating mat with rectal probe monitoring. The dorsal area was shaved and a full-thickness circular excisional skin wound of 12 mm diameter, including the panniculus carnosus, was created using a sterile biopsy punch (Acuderm Inc.). A sterilized donut-shaped silicone ring (1-mm thickness, 16-mm inner diameter, 24-mm outer diameter), prepared from transparent silicone sheets (Folioxane® Unrestricted, 0.5 x 90 x 150 mm, Novatech SA; Product no. FU050M; Batch no. 32226) using a 16- and 24-mm punch system (Facom, Morangis, France), was glued around the wound using silicone elastomer adhesive (Kwik-Sil Silicone Elastomer low viscosity glue, World Precision Instrument) to prevent wound contraction. Ten BVOs embedded in BC-ECM were implanted into the wound bed, covered with 150 µL cold liquid BC-ECM as described in Section 2.2, and overlaid with an Optiskin cover dressing (Laboratoires URGO; Product no. OPTISKIN FILM 10 cm × 12 cm; Batch no. 191205B). Upon contact with body temperature, the ECM polymerized and stabilized the implanted BVOs within the wound bed, and plaster strips were applied to secure the dressing and silicone ring. Animals were weighed twice weekly during dressing renewal and were observed daily for general condition, behavior, and mortality. The primary outcome measure was the presence or absence of implanted BVO-derived cells within the wound area at the endpoint. Animals were monitored in accordance with predefined humane endpoints and were euthanized if signs of suffering, toxicity, or excessive body weight loss were observed as defined in the study protocol. No animals were excluded from the analysis. Upon complete wound healing, mice were placed under deep gas anesthesia with isoflurane and euthanized by intraperitoneal injection of an overdose of pentobarbital (Euthasol® Vet., Dechra Veterinary Products SAS). A macroscopic autopsy was performed, and skin tissue from the wound area was collected, fixed in 4% paraformaldehyde for 24 hours, and

transferred to 1× PBS for storage. No statistical analysis was performed, as the objective was limited to determining the presence or absence of BVO-derived cells at the endpoint. All mouse experiments were conducted by ETAP-Lab (Nancy, France). The protocol was submitted via the AFiS online platform to the Comité d'Ethique Lorrain en Matière d'Expérimentation Animale (CELMEA, CEEA no. 066) on the 10th of October 2024 and received project authorization for the use of animals for scientific purposes from the French Ministry of Higher Education, Research and Innovation (approval no. APAFIS#51374) on the 28th of November 2024. All procedures were performed in compliance with 3R's ethical rules on animal experimentation.

2.6. Immunohistochemistry of skin wound sections

Skin wound tissues were processed for histological analysis by the Vienna BioCenter Core Facilities (VBCF). Following fixation, samples were dehydrated using an automated tissue processor (Donatello, Diapath) through a graded ethanol series (70%, 80%, 95%, and 99%) and xylene substitute (Epredia, #6764506) and subsequently embedded in molten paraffin.

Tissue blocks were manually oriented during embedding to ensure optimal sectioning of the wound area. Paraffin sections of 2 µm thickness were cut using a rotary microtome (HM355) and mounted onto glass slides (Surgipath Permaflex Plus). Sections were stretched in a warm water bath to minimize folding and dried overnight at 50 °C. For CD31 immunohistochemistry, slides were deparaffinized and rehydrated using an automated staining system (Gemini AS), followed by xylene substitute treatment, descending ethanol concentrations, and final equilibration in phosphate-buffered saline (PBS).

Antigen retrieval was performed manually by heat-induced epitope retrieval in citrate buffer for 30 minutes using a steamer, followed by cooling at room temperature for 15 minutes. Endogenous peroxidase activity was quenched using 3% hydrogen peroxide for 10 minutes. Sections were then washed in Tris-buffered saline (TBS) and blocked for 1 hour at room temperature in blocking solution containing 5% bovine serum albumin (BSA) and 10% goat serum in TBS with Tween-20 (TBS-T).

Primary antibody incubation was performed overnight at 4 °C using a mouse anti-human CD31 antibody (1:100 dilution in 5% BSA; ab9498). After washing (3 × 5 minutes in TBS-T), sections were incubated with a mouse linker antibody (1:500; ab133469) for 30 minutes at room temperature, followed by a rabbit enhancer (DCS Diagnostics Supervision 2 Polymer System) for 20 minutes and a rabbit polymer reagent for 30 minutes, with washing steps between each incubation.

Signal detection was achieved using 3,3′-diaminobenzidine (DAB) for 10 minutes. Slides were subsequently counterstained with hematoxylin, dehydrated, and cleared automatically using the Gemini AS system, and covered with Eukitt-neo mounting medium. Whole-slide imaging was performed using a Pannoramic Flash 250 scanner (20× objective, brightfield). Negative controls were generated by omission of the primary antibody and incubation with secondary antibody only.

2.7. Statistics

Statistical analyses were conducted using GraphPad Prism. Details of the statistical tests applied are provided in the figure legends. Data are presented as mean ± standard deviation (SD), unless stated otherwise. A p-value of 0.05 or less was considered statistically significant.

3. Results

3.1 Aggregation in 96 well Plates and Implementation of the "Sitting Drops" Method for ECM Embedding

Prior to initiating blood vessel organoid (BVO) formation, we first confirmed the pluripotency of the human induced pluripotent stem cells (hiPSCs) used in our experiments by assessing the expression of TRA 1-60 and SSEA-4 (Supp. Fig. 1A). We then aggregated hiPSCs in ultra-low attachment 6-well plates according to the standard protocol by Wimmer et al. (6). After seven days (after mesoderm and vascular induction), this approach resulted in multiple aggregates of varying sizes (Fig. 1A), which strongly influenced downstream differentiation efficiency. These size discrepancies significantly affected the ratio of endothelial (CD31-positive) and pericyte (PDGFRβ-positive) cells in mature (day 16) BVOs (Fig. 1B). Notably, smaller aggregates contained higher proportion of CD31-positive cells than large ones, and PDGFRβ-positive pericytes were nearly absent in aggregates with diameter between 100 µm and 200 µm. Aggregates smaller than 100 µm failed to develop into mature BVOs altogether.

To achieve uniform aggregate formation and improve differentiation consistency, we tested a range of commercially available plate types, some of them specifically designed for organoid culture. These included AggreWell 800 and SunBio plates, as well as various 96-well formats differing in well shape (U-bottom, flat-bottom) and surface coatings (ultra-low adhesion, delta surface, uncoated) (Fig. 1 D, Supp. Fig. 1B). Only the specialized aggregation plates (AggreWell 800 and SunBio plates) and U-bottom ultra-low attachment 96-well plates (ULU-96) generated single, compact aggregates per well after one day. However, only ULU-96 plates supported continuous and homogeneous growth during mesoderm and vascular induction (Fig. 1C). In contrast, aggregates in other formats either did not form properly, resulted in multiple irregular spheroids per well, or failed to grow consistently. Aggregates formed in ULU-96 plates maintained consistent size, spherical shape, and exerted stable morphology across all stages of differentiation (Fig. 1C, D).

Flow cytometric analysis further confirmed these observations. Aggregates cultured in ULU-96 showed markedly lower proportions of double-negative (CD31−/PDGFRβ−) cells (d7: 3.5±1.2%; d16: 1.6±0.9%) compared to those formed in AggreWell (d7: 82.1±1.8%; d16: 23.1±3.0%) or SunBio plates (d7: 75.0±8.0%; d16: 22.6±4.1%), indicating better differentiation efficiency (Fig. 1E, F; Supp. Fig. 1C-F). Other 96-well plate types produced irregular, poorly formed aggregates that lacked the size and structural integrity required for robust differentiation (Supp. Fig. 1B). Based on these

findings, we selected ULU-96 plates as the standard format for aggregate formation moving forward.

In the conventional two-layer protocol by Wimmer et al. (6), vascular networks are embedded at day 7 between two layers of a Matrigel- bovine collagen mix ECM (BC-ECM) in 12-well plates. However, we observed pronounced variability in cell composition when using Matrigel, consistent with its known batch-to-batch heterogeneity, leading to less reproducible endothelial-pericyte ratios (Supp. Fig. 1G). To overcome this limitation, we established Geltrex as a standardized ECM substitute for Matrigel based on its reproducible performance. While CD31 and PDGFRβ expression levels varied significantly across different Matrigel lots, Geltrex consistently supported stable differentiation of both endothelial and pericyte lineages (Supp. Fig. 1G) and was therefore adopted as our extracellular matrix of choice. Importantly, immunofluorescence staining confirmed that BVOs generated using Geltrex exhibited well-organized vascular networks containing CD31 and PDGFRβ positive cells, closely resembling those obtained with Matrigel (Fig. 1I, Supp. Fig. 1I).

To optimize the protocol and eliminate the excision step typically performed on day 12, we tested whether ECM embedding could be carried out directly in the ULU-96 aggregation plates. On day 7, following vascular induction, we removed the medium and applied 35 µL of Geltrex- BC-ECM directly onto the aggregates, allowing continued culture in the same wells without transferring the BVOs. We refer to this simplified embedding approach as the "sitting drop" method. ECM volumes ranging from 20-75 µL resulted in CD31 and PDGFRβ expression profiles (Supp. Fig. 1H) comparable to those of BVOs embedded using the conventional two-layer method (Fig. 1F). The ECM volume was carefully chosen so that by day 12, matrix digestion and contraction allowed the BVOs to detach naturally, eliminating the need for mechanical excision. Immunofluorescence and brightfield imaging confirmed the development of spherical organoids with vascular structures closely resembling those generated by the standard embedding protocol (Fig. 1H-J, Supp. Fig. 2A, B).

Low ECM volumes (≤20 µL) led to the generation of more compact organoids, whereas higher volumes (≥75 µL) resulted in loosely organized structures with reduced vessel network complexity and delayed spheroid maturation, extending up to day 30 (Supp. Fig. 2B).

We evaluated multiple 96-well plate types for ECM embedding of sitting drops and found that only ULU-96 plates consistently supported proper 3D development (Supp. Fig. 1J). By day 12, BVOs in alternative plate types developed dense, non-vascularized cores and failed to organize into vascular networks. A major advantage of ULU-96 plates is their compatibility with both aggregation and embedding steps, allowing the entire protocol to be executed in a single plate. This eliminates the need for manual transfers and significantly reduces variability and handling errors.

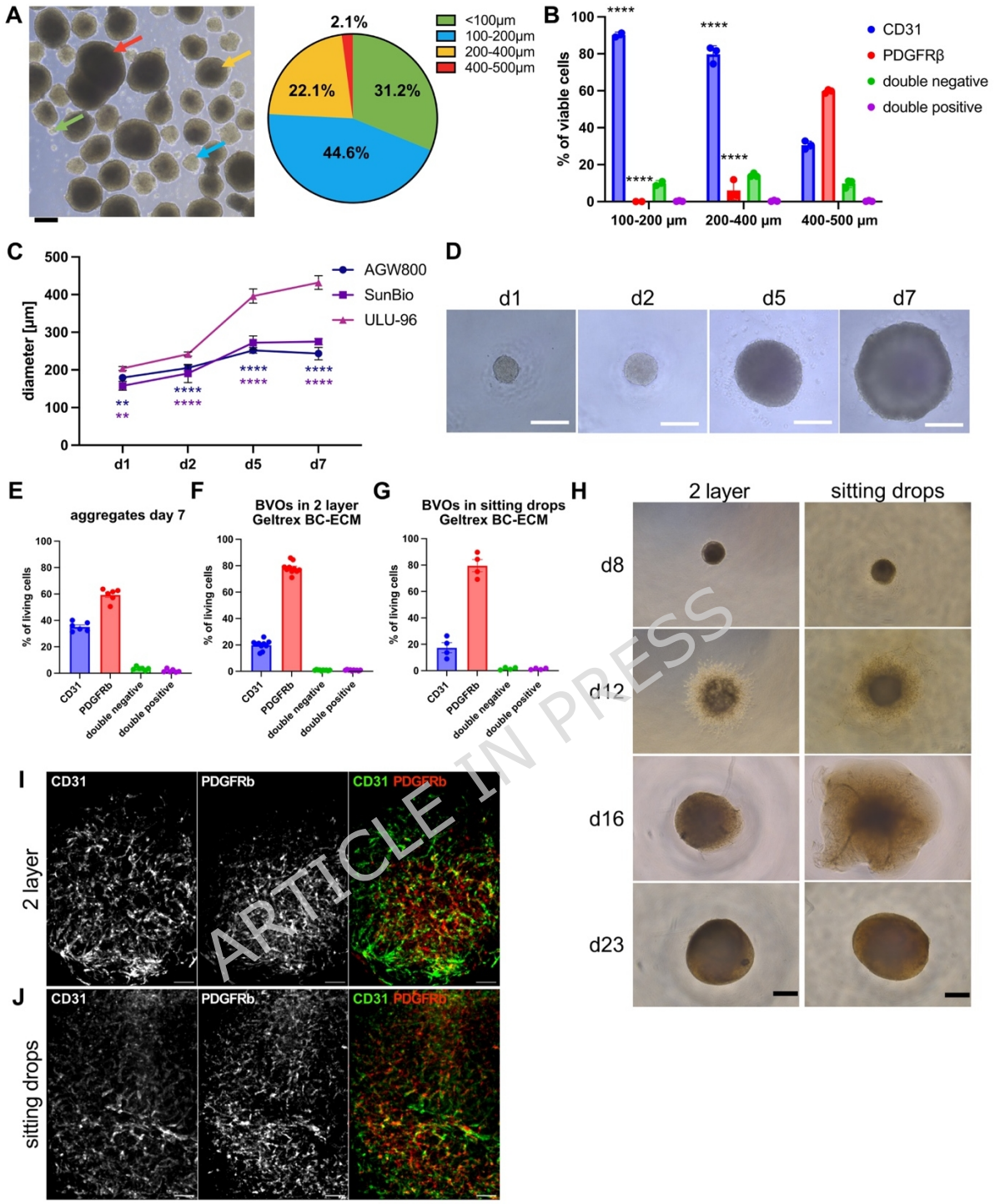

Figure 1. Optimization of blood vessel organoid (BVO) generation using ultra-low adhesion U-bottom 96-well plates. A: *Brightfield microscopy image (10x) of human induced pluripotent stem cell (hiPSC) aggregates with size classification on day 7. Scale bar: 250 µm. Colored arrows indicate representative aggregate sizes corresponding to the categories shown in the pie chart: green (<100 µm), blue (100-200 µm), yellow (200-400 µm), red (400-500 µm).* ***B:*** *Flow cytometry analysis of BVOs on day 16 showing endothelial cells (CD31⁺) and pericytes (PDGFRβ⁺). Prior to embedding, aggregates were size-fractionated by sieving, and BVOs were generated from aggregates of defined diameter (100-200 µm, 200-400 µm, 400-500 µm). Aggregates with diameter smaller than 100 µm did not develop into BVOs and were excluded from the analysis. All statistical comparisons were performed relative to the 400-500 µm group.* n *= 3 technical replicates. Statistical analysis: two-way ANOVA with Tukey's post hoc test.* ***C:*** *Comparison of aggregate growth in different culture plates: AggreWell 800 (AGW800), SunBio aggregation plate, and ultra-low attachment U-bottom 96-well plate (ULU-96). Aggregate diameters were measured on day 1 (post-aggregation), day 2 (prior to mesoderm induction), day 5 (prior to vascular induction), and on day*

7 (prior to embedding). Data from two independent experiments (4-5 technical replicates each). Statistical analysis: two-way ANOVA with Tukey's post hoc test. ***D:*** *Brightfield images (10x) of developing aggregates in ULU-96 plates from day 1 to day 7 (same time points as in C). Scale bar: 200 µm.* ***E-G:*** *Flow cytometry analysis of CD31⁺ and PDGFRβ⁺ populations in (E) aggregates on day 7 (*n *= 6 biological replicates), (F) BVOs embedded in two layer Geltrex-bovine collagen mix ECM (BC-ECM) on day 16 (*n *= 4 biological replicates), and (G) BVOs cultured in Geltrex- BC-ECM as sitting drops in ULU-96 plates until day 23 (*n *= 4 biological replicates).* ***H:*** *Brightfield images (4×) showing development of BVOs embedded in Geltrex- (BC-ECM) as two-layer versus sitting drops cultures in ULU-96 plates on days 8, 12, 16, and 23. Scale bar: 500 µm.* ***I, J:*** *Immunofluorescence staining (10x) of BVOs on day 16. (I) BVOs were generated using the two-layer Geltrex- BC-ECM protocol or (J) the sitting drop method in ULU-96 plates with Geltrex- BC-ECM, and stained for CD31 (green) and PDGFRβ (red). Single-channel and merged images are shown. Scale bar: 100 µm. **p □ 0.01; ***p □ 0.001.*

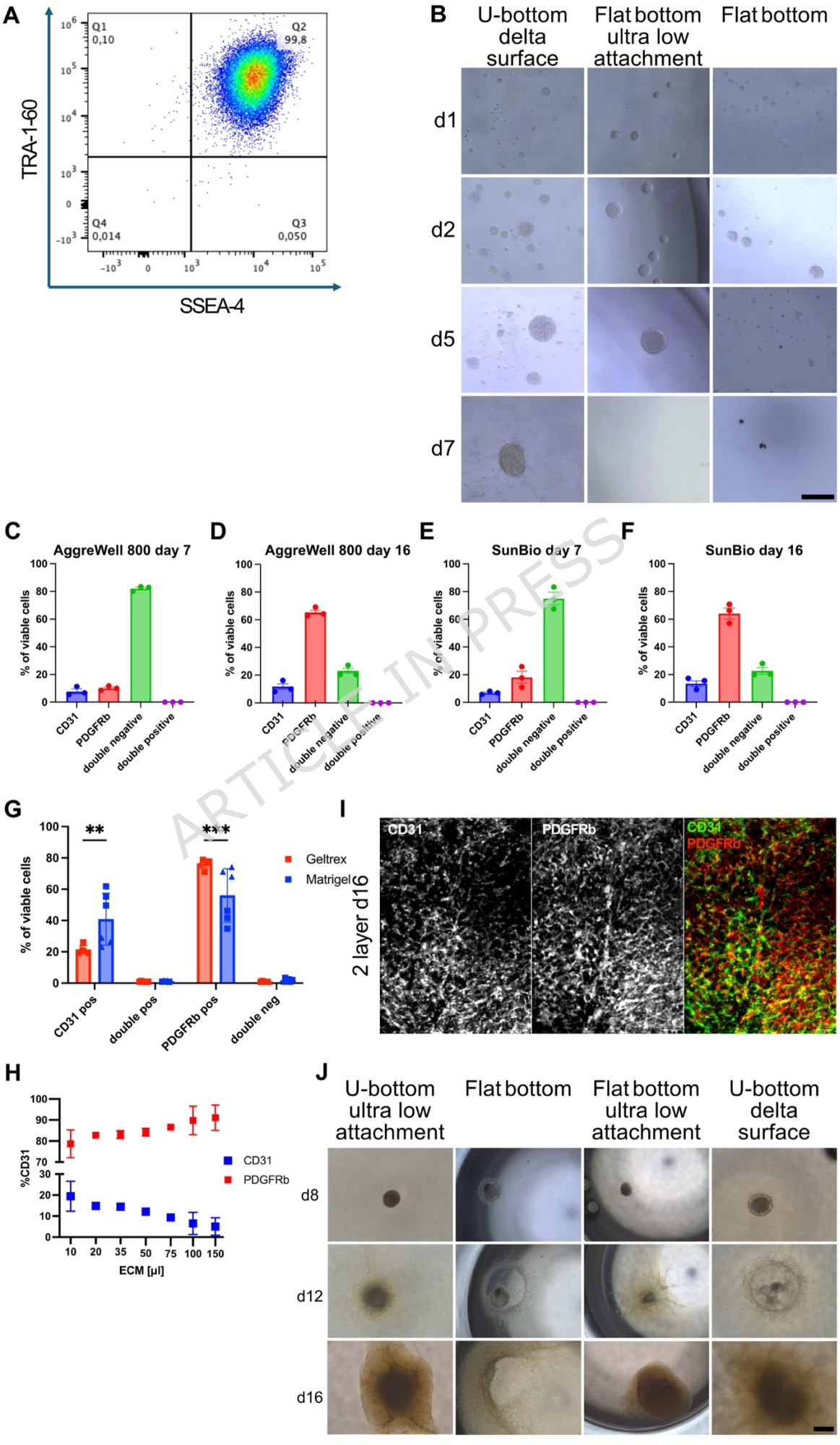

Supplemental Figure 1. Supporting data for hiPSC pluripotency, plate testing, and BVO optimization. ***A:*** *Flow cytometry analysis confirming pluripotency of hiPSCs prior to aggregation (day 0). Cells were stained for SSEA-4 and TRA-1-60.* ***B:*** *Brightfield microscopy images (10x) of cell aggregates cultured in different 96-well plate formats: delta surface U-bottom plates, flat-bottom ultra-low attachment plates, and standard flat-bottom plates. Images were taken on day 1 (post-aggregation), day 2 (prior to mesoderm induction), day 5 (prior to vascular induction), and day 7 (prior to embedding). Scale bar: 200 µm.* ***C-F:*** *Flow cytometry analysis of endothelial cells (CD31, blue), pericytes (PDGFRβ, red), double-positive cells (purple), and double-negative cells (green). (C) BVOs were generated using AggreWell 800 before embedding on day 7 and (D) after culture until day 16, or (E) using SunBio plates before embedding on day 7 and (F) after culture until day 16.* n *= 3 technical replicates per condition.* ***G:*** *Flow cytometry comparison of BVOs at day 16 generated with Geltrex- bovine collagen mix extracellular matrix (BC-ECM) (red) versus Matrigel- BC-ECM (blue). CD31⁺, PDGFRβ⁺, double-positive, and double-negative populations are shown. Data from two independent differentiation experiments (biological replicates), each performed with three technical replicates. Different symbols (square and circles) indicate independent biological replicates. Each biological replicate used an independently thawed Matrigel lots. Statistical analysis: two-way ANOVA with Tukey's post hoc test.* ***H:*** *Flow cytometry quantification of CD31⁺ and PDGFRβ⁺ cells in BVOs formed in ULU-96 plates, cultured with varying ECM volumes. BVOs were analyzed after reaching a spherical stage. Data represent 2 biological replicates.* ***I:*** *Immunofluorescence staining (10x) of BVOs on day 16, generated using the two-layer Matrigel-BC-ECM protocol and stained for CD31 (green) and PDGFRβ (red). Single-channel and merged images are shown. Scale bar: 100 µm.* ***J:*** *Brightfield microscopy images (4x) of BVOs embedded in 35 µL Geltrex- BC-ECM using the sitting drop method and cultured in ultra-low attachment U-bottom plates, standard flat-bottom plates, flat-bottom ultra-low attachment plates and delta-surface U-bottom plates. Images were taken on days 8, 12, and 16. Only BVOs in ULU-96 plates maintained a three-dimensional structure; in other plates, dense cores formed by day 12. Scale bar: 500 µm. **p □ 0.01; ***p □ 0.001.*

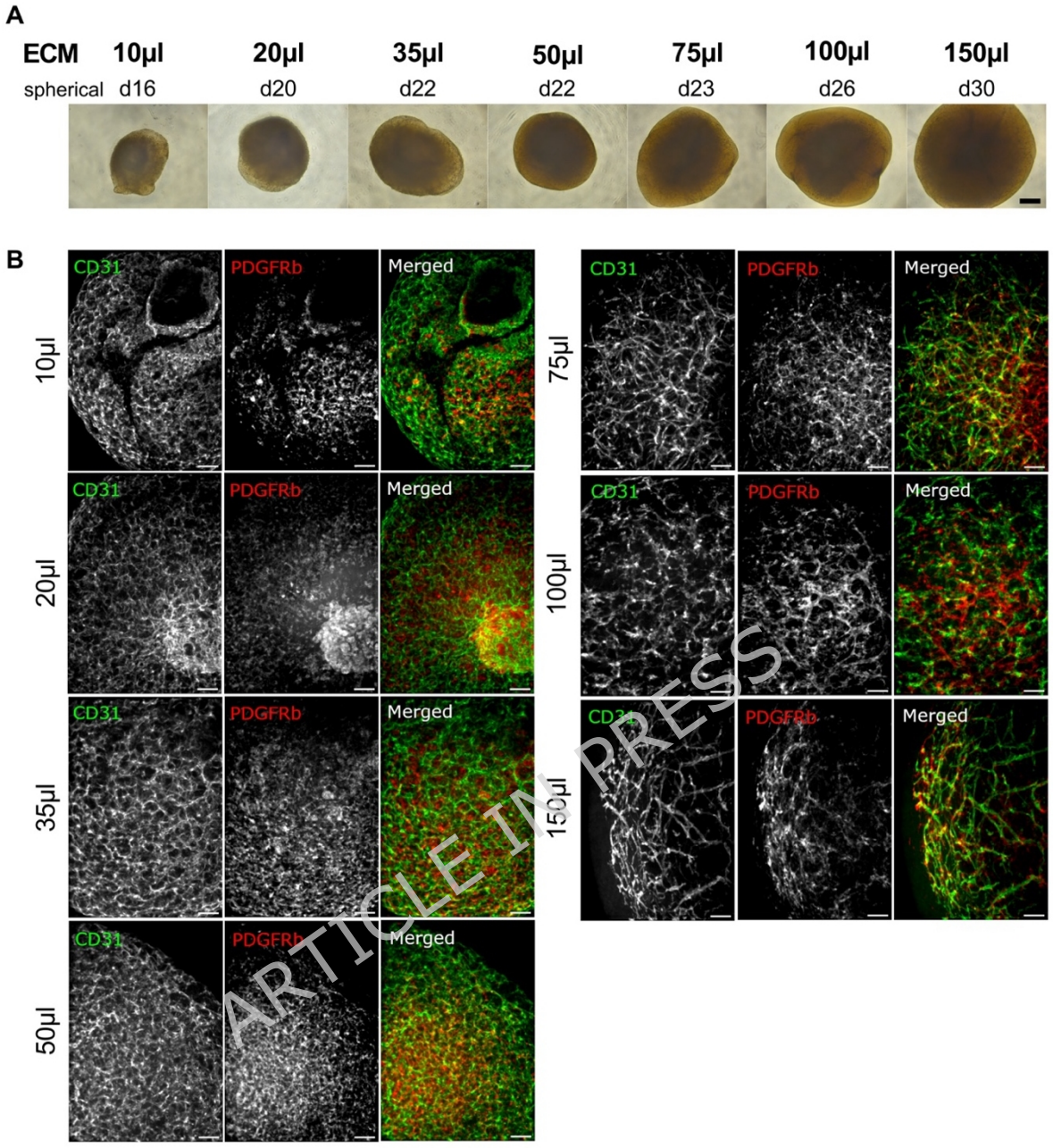

Supplemental Figure 2. Development of BVOs using the sitting drop method in different volumes of extracellular matrix (ECM)*. **A:** Brightfield microscopy images (4x) of BVOs using the sitting drops method embedded in a Geltrex- bovine collagen (BC-ECM) mix. Sitting drops were cultured in different ECM volumes ranging from 10 µL to 150 µL. The day at which each BVO reached a spherical morphology is indicated above the respective image. Spherical morphology was determined by daily visual inspection and defined as the time point at which the surrounding extracellular matrix was no longer detectable and the organoid appeared as a free-floating, compact, spherical structure by visual inspection. Scale bar: 500 µm. **B:** Immunofluorescence staining (10x) of BVOs using the sitting drops method after they got spherical, embedded in a Geltrex- BC-ECM. Sitting drops were cultured in different ECM volumes ranging from 10 µL to 150 µLand stained for CD31 (green) and for PDGFRβ (red). Single channels and merged images are shown. Scale bar: 100 m.*

3.2 Generation of BVOs in a defined, Matrigel-/Geltrex-Free ECM

Matrigel and Geltrex are complex, animal-derived extracellular matrices that exhibit considerable batch-to-batch variability and have limited translational relevance (11, 12). To address these limitations, we established a method for generating BVOs using a defined ECM, free of both Matrigel and Geltrex. Aggregates were embedded in ULU-96 plates using 2.15 mg/mL final concentration of bovine-collagen (PureCol) as the sole source of collagen I (BC-ECM), with 35 µL of ECM applied per sitting drop.

By day 16, BVOs generated in bovine-collagen ECM (BC-ECM) sitting drops displayed morphological features indistinguishable from those embedded in Geltrex- BC-ECM sitting drops, including a uniform spherical shape and homogeneous structure (Fig. 2A). Because the ECM in bovine-collagen cultures was not fully degraded by day 16, we extended the culturing period to day 23. At that point, the matrix was completely digested, and the BVOs had matured into compact, spherical structures (Fig.2A, F).

Flow cytometry analysis revealed that the cellular composition of BVOs at day 23 grown in BC-ECM sitting drops closely resembled that of Geltrex-BC-ECM derived BVOs (Fig. 2C, D). Extending the culture from day 16 to day 23 had no impact on the cell composition in either condition (Fig. 2B-D, Fig. 1G), indicating high stability of mature BVOs. Morphologically, BVOs grown in BC-ECM at both time points were comparable to those generated in Geltrex- BC-ECM (Fig. 2E, F; Fig. 1I, J). Notably, immunofluorescence staining of BC-ECM sitting drops derived BVOs at day 23 revealed a slightly improved structural organization with more distinct vascular patterns (Fig. 2F). These findings demonstrate the feasibility of generating BVOs in a defined, Matrigel- and Geltrex-free ECM.

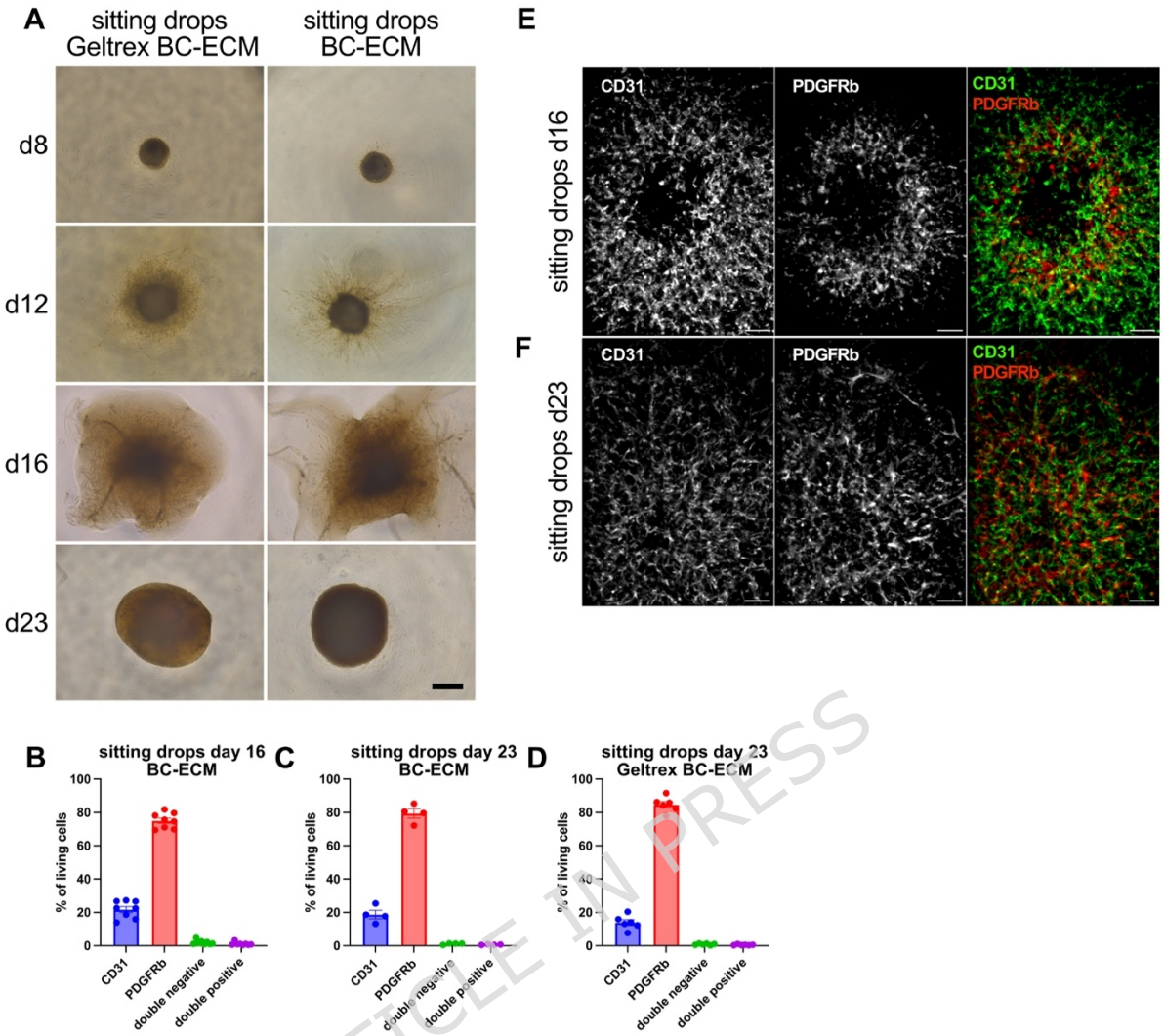

Figure 2. Generation of blood vessel organoids (BVOs) in a defined bovine collagen extracellular matrix (BC-ECM). *__A:__ Brightfield microscopy images (4x) comparing development of BVOs (sitting drops) embedded in bovine collagen (BC-ECM) versus Geltrex-BC-ECM. Images were taken on days 8, 12, 16, and 23. BVOs in both ECM types developed a similar spherical morphology over time. Scale bar: 500 µm. __B:__ Flow cytometry analysis of BVOs (sitting drops) embedded in BC-ECM at day 16, showing proportions of endothelial cells (CD31⁺, blue), pericytes (PDGFRβ⁺, red), double-negative (green), and double-positive (purple) populations.* n = *4 biological replicates with 2 technical replicates each. __C:__ Flow cytometry analysis of BVOs (sitting drops) in BC- ECM at day 23. Cell composition remained comparable to day 16.* n = *4 biological replicates. __D:__ Flow cytometry analysis of BVOs (sitting drops) embedded in Geltrex- BC-ECM at day 23.* n = *4 biological replicates. __E, F:__ Immunofluorescence staining (10x) of BVOs generated as single-layer sitting drops in ULU-96 plates with BC-ECM, shown at day 16 (E) and day 23 (F). Samples were stained for CD31 (green) and PDGFRβ (red); single-channel and merged images are shown. Scale bar: 100 µm.*

3.3 Generation of BVOs in Animal-origin-free ECM

To support the potential clinical application of BVOs in cell-based therapies and personalized medicine, it is essential to transition toward animal-origin-free culture conditions. Eliminating animal-derived components improves experimental reproducibility, minimizes the risk of contamination, and aligns with current regulatory and ethical standards. Moreover, animal-origin-free systems support safer, more standardized, and sustainable production processes.

To this end, we generated BVOs using commercially available recombinant human collagen type I as the sole component of the ECM. Aggregates were cultured in ULU-96 plates and embedded in 35 µL human collagen ECM (HC-ECM) per sitting drop. Human collagen concentrations between 1 and 5 mg/mL yielded reproducible polymerization behavior and resulted in structurally stable BVOs (Supp. Fig. 3A-C). Flow cytometry analysis confirmed consistent formation of both endothelial ($CD31^+$) and pericyte ($PDGFR\beta^+$) populations across all conditions (Supp. Fig. 3A), with statistically significant but moderate differences, such as a lower proportion of $PDGFR\beta^+$ cells at 3.5 and 5 mg/mL compared to 2 mg/mL. In addition, BVOs cultured in higher collagen concentrations required longer culture times to reach a compact spherical morphology compared to those embedded in 2 mg/mL collagen (Supp. Fig. 3B). Immunofluorescence staining further confirmed the presence of $CD31^+$ endothelial networks and $PDGFR\beta^+$ pericytes under all conditions (Supp. Fig. 3C). To quantitatively compare organoid morphology across ECM conditions, Feret diameter measurements were performed at the spherical stage (Supp. Fig. 3D). BVOs embedded in 2 mg/mL collagen displayed the most consistent size distribution (mean ± SD: 1192 ± 116 µm), whereas lower collagen concentration resulted in smaller organoids (1 mg/mL: 803 ± 132 µm). Increasing collagen concentrations led to progressively larger and more heterogeneous organoids (3.5 mg/mL: 1282 ± 264 µm; 5 mg/mL: 1617 ± 321 µm).

BVOs formed in human collagen (2 mg/mL) (Fig. 3A) exhibited typical organoid architecture at both day 16 and day 23 (Fig. 3 B, C) and maintained stable proportions of $CD31^+$ endothelial and $PDGFR\beta^+$ pericyte populations over time, with no notable changes in cell type composition between the two time points (Fig. 3D, E). Endothelial cells ($CD31^+$) and Pericytes ($PDGFR\beta^+$) displayed comparable spatial distribution across individual organoids from different differentiation experiments (Supp. Fig. 4A, B). Based on consistent size, preserved cellular composition, and faster acquisition of spherical morphology, 2 mg/mL human collagen was selected as the standard concentration for animal-origin-free ECM condition. It is worth noting though that across all tested human collagen concentrations, BVOs retained similar endothelial and pericyte populations and typical organoid architecture, indicating that human collagen type I supports robust BVO formation under animal-origin-free conditions.

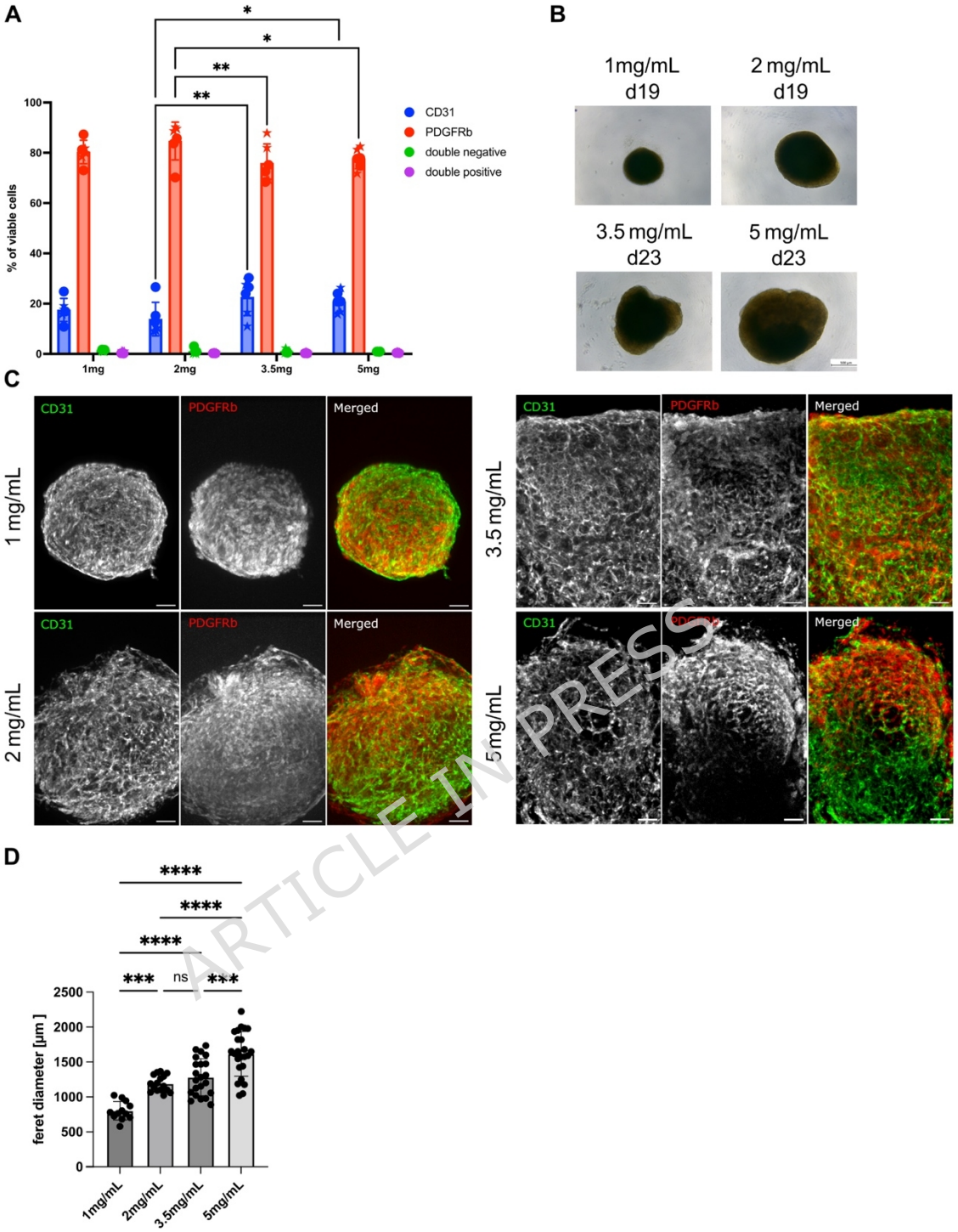

Supplemental Figure 3. Development of blood vessel organoids (BVOs) using the sitting drop method in different concentrations of human collagen ECM (HC-ECM). ***A****: Flow cytometry quantification of CD31⁺ and PDGFRβ⁺ cells in BVOs formed in ULU-96 plates using varying human collagen concentrations in the ECM. Sitting drops were cultured in different human collagen concentrations ranging from 1 mg/mL to 5mg/mL. BVOs were analyzed after reaching a spherical stage. Data represents 3 technical replicates. Statistical analysis: two-way ANOVA with Tukey's post hoc test.* ***B****: Brightfield microscopy images (4x) of BVOs (sitting drops) embedded in HC-ECM. The day on which each BVO reached a spherical morphology is indicated above the respective image. Scale bar: 500 µm.* ***C:*** *Immunofluorescence staining (10x) of BVOs formed in ULU-96 plates using varying human collagen concentrations in the ECM upon reaching spherical appearance. BVOs were stained for CD31 (green) and for PDGFRβ (red). Single channels and merged images are shown. Scale bar: 100 µm.* ***D:*** *Quantitative analysis of organoid size across increasing collagen concentrations (1, 2, 3.5, and 5 mg/mL). Feret diameter measurements were performed at the spherical stage. Data represent* n *= 12–24 organoids per condition from* N *= 2*

*independent experiments. Statistical significance was assessed by one-way ANOVA followed by Tukey's multiple comparisons test. *p ≤ 0.05**, p ≤ 0.01, ***p ≤ 0.001; ****p ≤ 0.0001, ns: not significant.*

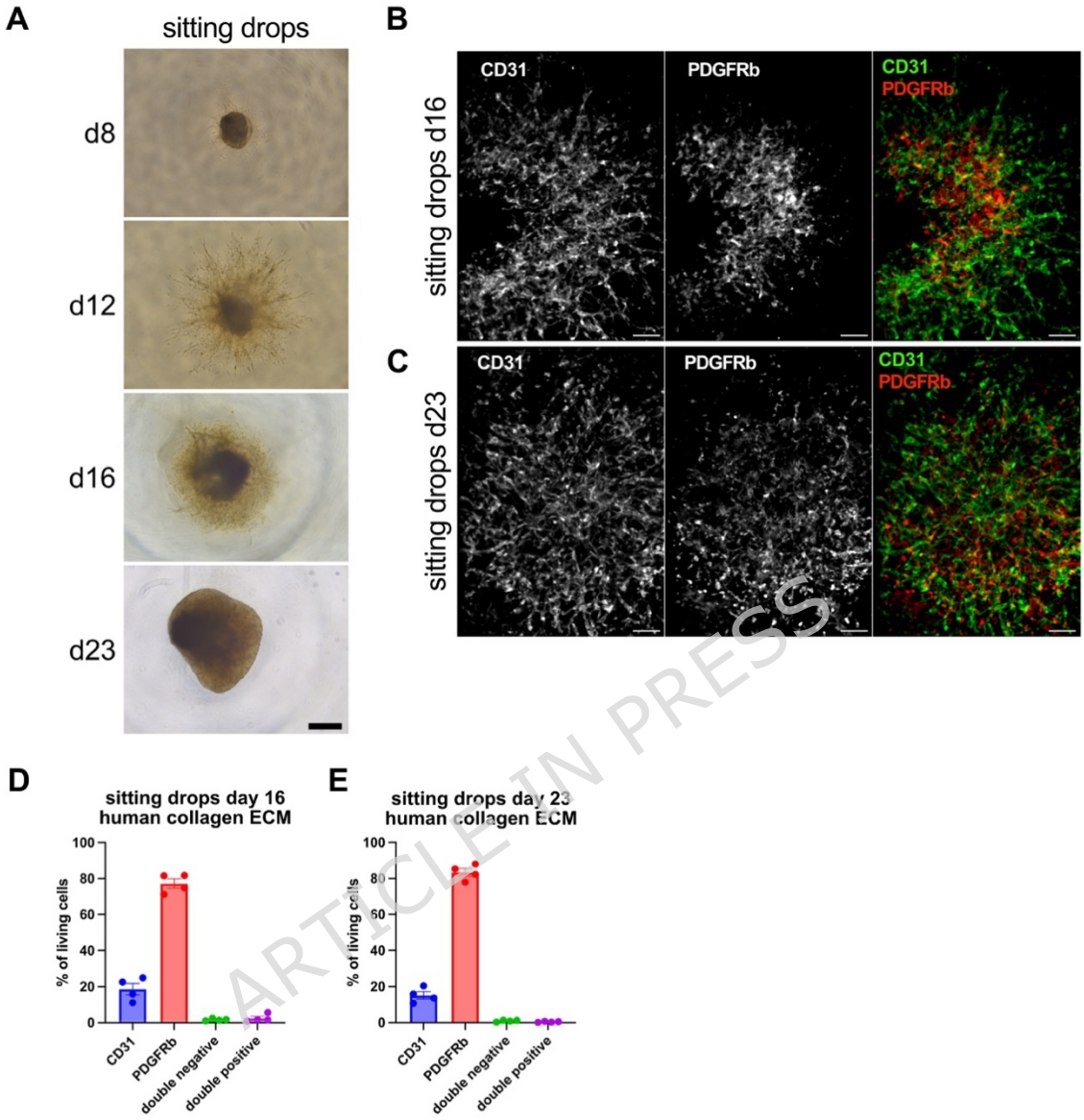

Figure 3. Generation of animal-origin-free blood vessel organoids (BVOs) using 2mg/mL recombinant human collagen I.
A: *Brightfield microscopy images (4x) of BVOs embedded in 2 mg/mL of human collagen ECM (HC-ECM) using the sitting drop method in ultra-low attachment U-bottom 96-well (ULU-96) plates. Images were taken on days 8, 12, 16, and 23. Scale bar: 500 µm.* ***B, C:*** *Immunofluorescence staining (10x) of BVOs embedded in 2 mg/mL of HC-ECM using the sitting drop method and cultured in ULU-96 plates, imaged at day 16 (B) and day 23 (C). Samples were stained for CD31 (green) and PDGFRβ (red); single-channel and merged images are displayed. Scale bar: 100 µm.* ***D, E:*** *Flow cytometry analysis of BVOs embedded in 2 mg/mL of HC-ECM using the sitting drop method at day 16 (D) and day 23 (E), showing proportions of endothelial cells (CD31⁺, blue), pericytes (PDGFRβ⁺, green), double-positive cells (red), and double-negative cells (purple). Cell composition remained stable over time.* n = *4 biological replicates.*

3.4 Functional Testing of BVOs generated in sitting drops *in vivo*

To evaluate the functionality of BVOs generated in BC-ECM (2.15 mg/mL PureCol) as sitting drops, we implanted them into full-thickness skin wounds of non-obese diabetic severe combined immunodeficiency (NOD SCID gamma) mice. BVOs remained within the wound environment for a period of 32 days, during which extensive tissue remodeling and vascular regeneration occurred. After complete wound closure, skin samples were excised and subjected to immunohistochemical analysis using a human-specific CD31 antibody to assess the fate of BVO-derived endothelial cells. Immunohistochemical analysis revealed human CD31-positive cells within vascular structures in the healed wound tissue. These human CD31-positive cells were found in association with host-derived vascular cells, forming chimeric vessel structures. (Fig. 4, Suppl. Fig. 5 A)**.** An overview of the healed wound architecture and the anatomical localization of the analyzed regions is provided in Supplemental Figure 5B. In some cross-sections of such chimeric vessels, erythrocytes were detected within the lumen (Supp. Fig. 5 A, blue arrow), consistent with integration of BVO-derived endothelial cells into host blood vessels.

Notably, implanted BVOs were no longer detectable as intact, self-contained organoid structures at the time of analysis, suggesting that organoid-derived cells dispersed and integrated into the regenerating host tissue during the wound healing process.

While functional perfusion of organoid-derived vascular networks was not directly assessed, the presence of BVO-derived human endothelial cells within newly formed host blood vessels indicates a contributory role of these cells in host neovascularization during wound healing.

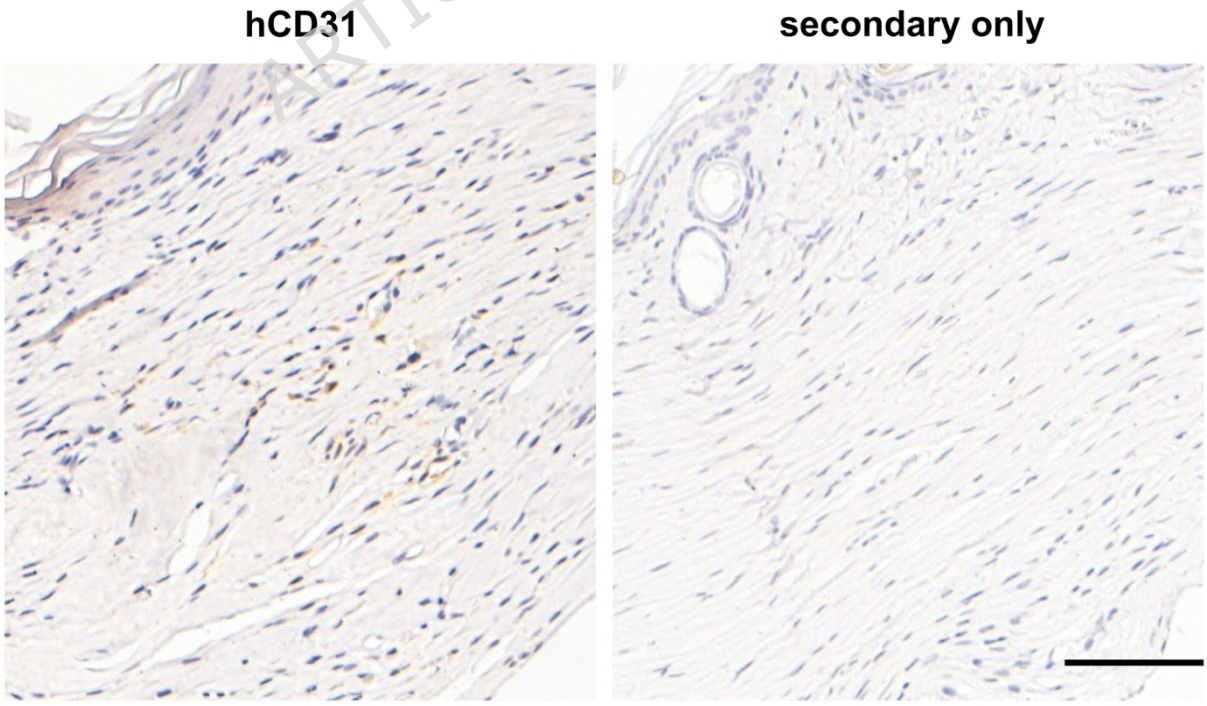

Figure 4. ***Integration of BVO-derived human endothelial cells into host vasculature following implantation into a mouse skin wound model.*** *Blood vessel organoids (BVOs) generated via the sitting drop method were implanted into full-thickness skin wounds of*

immunodeficient mice and remained in the wound environment for 32 days until complete wound closure. Tissue sections were collected and analyzed by immunohistochemistry using a human-specific CD31 antibody. Human CD31-positive cells were detected within vascular structures of the healed wound tissue, frequently in association with host-derived cells. A secondary-antibody-only control is shown to confirm staining specificity. Scale bar: 100 µm.

4 Discussion

The development of cell-based therapies represents a significant advancement in medical research. Organoid technologies, including patient-derived and allogeneic systems, are increasingly utilized for diagnostics, disease modeling, and as autologous grafts for regenerative therapies (13, 14). Blood vessel organoids (BVOs), in particular, offer a promising platform to support vascular repair, wound healing, and tissue regeneration due to their structural and functional resemblance to native vasculature (7).

Existing BVO production protocols are resource-intensive, laborious, and poorly suited for high-throughput applications (6, 7, 15, 16). A key limitation lies in the widespread use of animal-derived extracellular matrices such as Matrigel and Geltrex, which suffer from batch-to-batch variability, undefined composition, and lack of GMP compliance (11, 12). These properties restrict reproducibility and clinical applicability, posing regulatory and ethical challenges. Recent advances in organoid culture emphasize the need for defined, synthetic, or recombinant ECMs to overcome these challenges (17). Various animal-origin-free substrates can potentially provide viable support for pluripotent stem cell culture. A recent publication (18) identified Vitronectin as such promising animal-origin-free substrate for maintaining hiPSC pluripotency. In our experience, Laminin-521-a fibrous protein present in the basement membrane- reliably preserved pluripotency over multiple passages and therefore provided a stable starting point for downstream differentiation. The successful use of fibrin gel as an ECM in the same study (18), albeit more complicated and less viable for large scale utilization, outlines that there are further alternatives to animal-origin-free ECM substrates. Notably, we agree with the authors' observations regarding the limited suitability of several commercially available hydrogel systems (18), which underscores the narrow range of biochemical and mechanical ECM properties compatible with vascular organoid differentiation

In this study, we developed and validated an optimized and clinically relevant protocol for BVO generation using defined, animal-origin-free extracellular matrices (Fig. 5). By performing the entire process, from aggregation to organoid maturation, within a single ultra-low attachment 96-well plate, we reduced manual handling and contamination risk while enabling compatibility with robotic liquid handling platforms. This streamlined workflow allows for standardized large-scale production and facilitates the implementation of high-throughput drug testing. Compared to the widely used two-layer protocol by Wimmer et al. (6), our method eliminates excision steps, uses fewer reagents, and offers a simplified one-step ECM embedding procedure.

BVOs generated using this platform showed consistent morphology and a stable composition of $CD31^+$ endothelial cells and $PDGFR\beta^+$ pericytes across different ECM types and culture durations. Immunofluorescence imaging confirmed comparable vascular organization between BVOs produced in Geltrex/Matrigel- and collagen-only-based matrices. Importantly, we demonstrate that recombinant human collagen type I is sufficient to support robust organoid formation, enabling a fully animal-origin-free workflow and GMP-compatible production. Across the tested concentration range (1-5 mg/mL), endothelial and pericyte differentiation remained stable, with statistically significant but moderate differences in $CD31^+$ cell proportions at 3.5 and 5 mg/mL compared to 2 mg/mL. These findings highlight that the protocol is tolerant to collagen concentration variations within the ECM while maintaining reproducibility, which is critical for clinical translation.

In the skin wound model, transplanted BVOs did not persist as intact organoid structures but instead appeared to undergo extensive remodeling within the wound environment. Given the prolonged implantation period of 32 days, during which dynamic tissue regeneration and vascular restructuring take place, it is not unexpected that discrete organoid structures were no longer detectable at the time of analysis. Rather, BVO-derived human endothelial cells were found to integrate into the host vascular network. While we did not specifically teste for the successful integration of BVO-derived human pericytes, we would expect that these calls could also integrate into the host vasculature.

Despite these advances, challenges remain. Polymerization behavior and mechanical properties of collagen-based ECMs can vary between lots and suppliers, potentially affecting reproducibility. Continued optimization and standardization of collagen formulations will be essential for scaling up production. Furthermore, integrating real-time monitoring and closed-loop feedback systems into automated workflows could enhance quality control for large-scale manufacturing (19).

While our attempts of using AggreWell or SunBio plates for the aggregation step resulted in suboptimal growth and an unfavorable CD31:PDGFRβ ratio in our hands, it is worth noting that other groups have reported successful aggregation and BVO generation using microwell platforms such as the AggreWell system (20, 21). Nevertheless, this did not limit our workflow, because the single ultra-low-attachment 96-well plate used here offers superior performance and significantly simplifies handling by eliminating transfers between plates.

Finally, emerging bioengineering technologies such as microfluidic platforms, 3D bioprinting and multi-organoid assembloids provide additional opportunities to enhance vascular architecture and complexity and integration (22-24). Combining our protocol with patient-specific iPSC lines could pave the way for individualized vascular organoids in disease modeling, drug screening, and ultimately autologous cell- based therapies.

In summary, we present a robust and efficient method for generating BVOs in a single-plate format using GMP-compatible and animal-origin-free components. The sitting drop technique simplifies the workflow, supports high-throughput scalability, and provides a foundation for clinical translation of vascular organoid technologies.

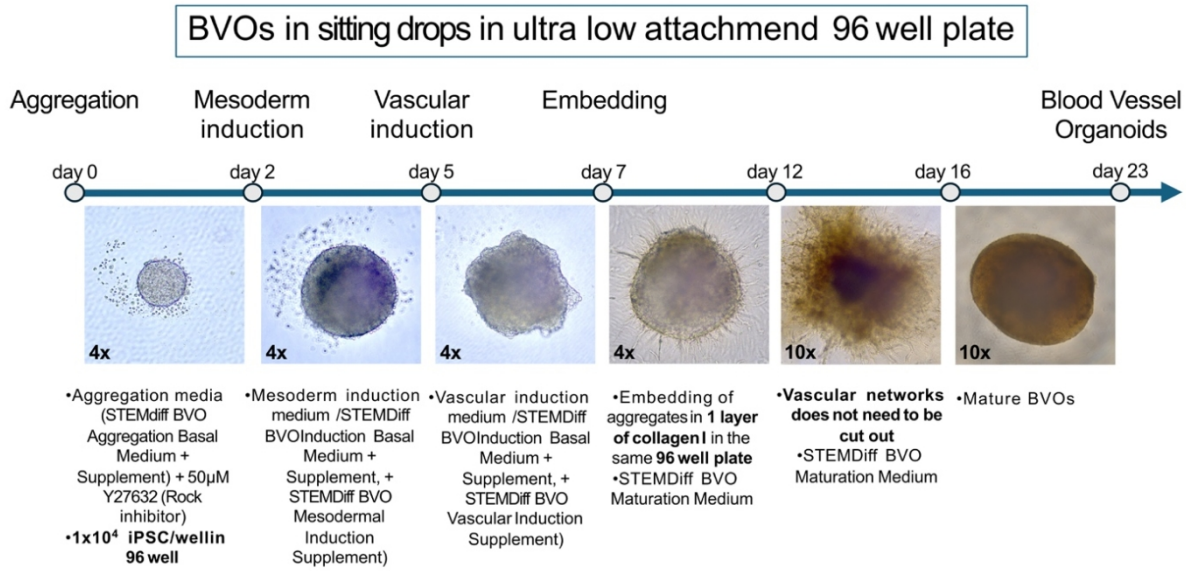

Figure 5 Schematic overview of the blood vessel organoid (BVO) generation protocol using the sitting drop method. *Timeline representation of the BVO differentiation protocol performed in ultra-low attachment U-bottom 96-well plates. The scheme outlines each step of the process, including aggregation, mesoderm induction, vascular induction, and maturation, together with the corresponding reagents and media used at each time point. Representative brightfield images illustrate the progression of BVOs from day 1 (aggregation) to day 23 (mature organoid). The timeline highlights the standardized workflow and practical implementation for robust and reproducible BVO generation. Magnification is indicated in the bottom left corner of each image.*

5 Conclusion

In summary, our study presents a novel, efficient, and robust protocol for the generation of blood vessel organoids. By eliminating animal-origin-derived components and simplifying the culture process, this approach offers a scalable and clinically relevant platform for organoid-based applications. Future work will focus on further optimizing the system for therapeutic use, including disease modeling, drug screening, and regenerative medicine.

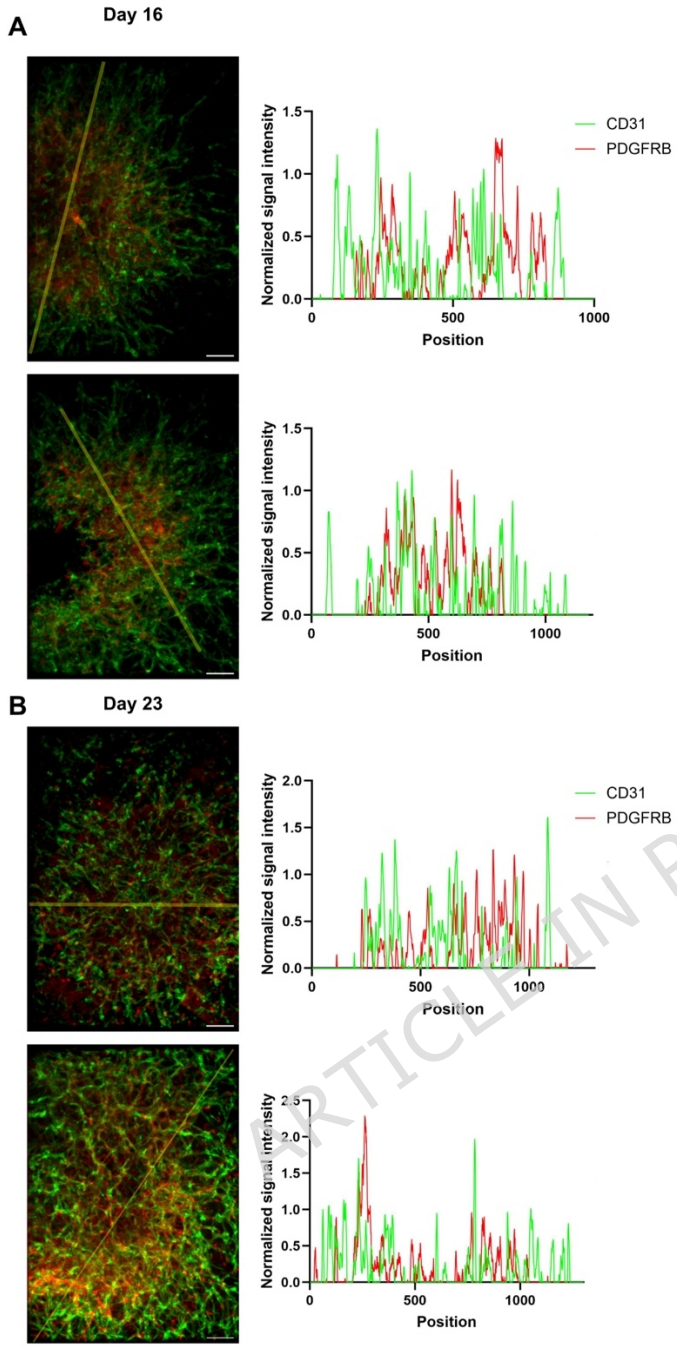

Supplemental Figure 4. Spatial distribution of endothelial and pericyte markers in blood vessel organoids generated in human collagen ECM. (A) *Representative immunofluorescence images of blood vessel organoids (BVOs) generated in recombinant human collagen I ECM (2 mg/mL) and analyzed at day 16. (B) Corresponding images of BVOs analyzed at day 23. Organoids were stained for the endothelial marker CD31 (green) and the pericyte marker PDGFRβ (red). The yellow line indicates the region of interest (ROI; 10-pixel width) used for line-based intensity profiling across the organoid. Normalized signal intensities for CD31 and PDGFRβ along the ROI are plotted as a function of position, providing a quantitative representation of the spatial distribution of endothelial and pericyte signals in addition to the immunofluorescence images. The thinner appearance of the ROI line in the second image in (B) reflects acquisition at higher image resolution. Scale bar: 100 µm.*

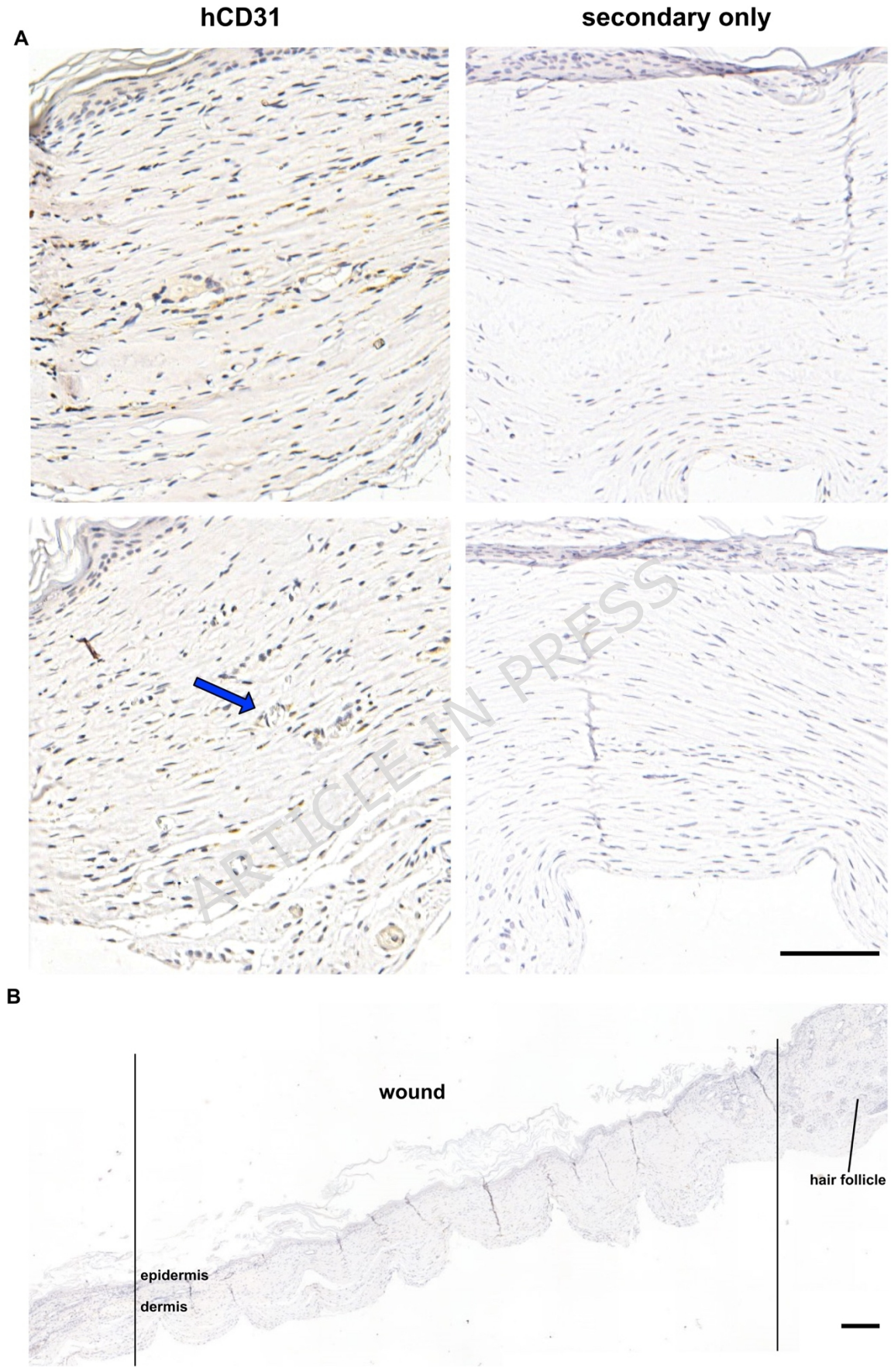

Supplemental Figure 4. Immunohistochemical analysis and anatomical context of healed mouse skin wounds following BVO implantation*. **(A)** Representative additional images of immunohistochemical staining for human CD31 in healed mouse skin wounds 32 days after*

implantation of blood vessel organoids (BVOs). Human CD31-positive cells are detected within vascular structures of the wound tissue. A cross-section of a hybrid vessel containing erythrocytes within the lumen is indicated by the blue arrow. Secondary-antibody-only controls are shown to confirm staining specificity. Scale bar: 100 µm. ***(B)*** *Low-magnification overview of a healed full-thickness skin wound. The wound center is identifiable by a thinner dermis lacking hair follicles, while the wound margins are characterized by the reappearance of hair follicles and thicker epidermal layers. Scale bar: 200 µm.*

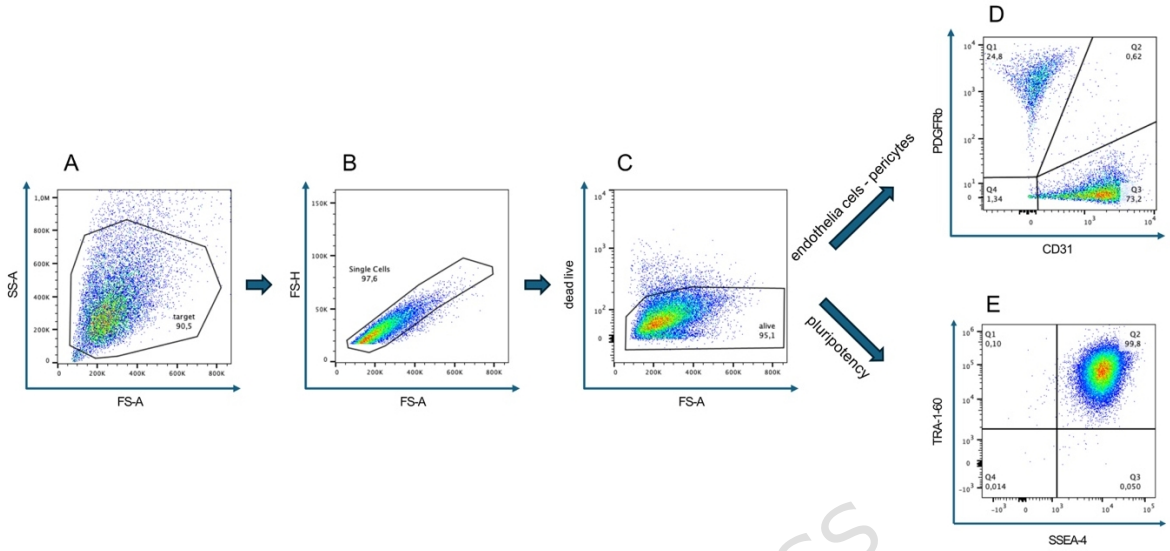

Supplemental Figure 6. Flow cytometry gating strategy. A-B: *Representative plots showing the gating strategy. (A) Debris, (B) doublets and (C) dead cells were excluded from the analysis.* ***D-E:*** *Viable cells from C were either analyzed for (D) endothelial (CD31) and pericyte (PDGFRβ) marker expression in vascular networks (day7) and mature organoids or (E) pluripotency (TRA-1-60 and SSEA-4) marker expression in induced pluripotent stem cells or at later stages of differentiation to confirm their absence.*

Author Contribution

A.H as first author designed and performed experiments, carried out the statistical analyses and wrote the manuscript. D.S. and J.T. designed and performed experiments and contributed to the writing of the manuscript. Y.H.T. performed image analysis. J.F.B. contributed to the mouse experiment. T.E.Y. initiated and supervised the project, designed experiments and wrote the manuscript as corresponding author.

Acknowledgements

The authors would like to thank Sophia Wedel and Maria Dumitrascuta for their excellent preliminary work that formed the basis of this manuscript. We further acknowledge the Tiroler Krebsforschungsinstitut (TKFI) for their generous support and for providing access to their facilities and equipment.

Conflict of Interests

The authors declare no conflict of interests.

Data availability

The data, presented in this study, are available from the corresponding author on reasonable request.

Funding

Standortagentur Tirol, Health Hub grant, TAM: TM-12514133
Austrian Research Promotion Agency (FFG), Project Number: FO999925858
European HORIZON, Grant agreement ID: 101135053

References

1. Sato T, Vries RG, Snippert HJ, van de Wetering M, Barker N, Stange DE, et al. Single Lgr5 stem cells build crypt-villus structures in vitro without a mesenchymal niche. Nature. 2009;459(7244):262-5.
2. Huch M, Dorrell C, Boj SF, van Es JH, Li VS, van de Wetering M, et al. In vitro expansion of single Lgr5+ liver stem cells induced by Wnt-driven regeneration. Nature. 2013;494(7436):247-50.
3. Sachs N, Papaspyropoulos A, Zomer-van Ommen DD, Heo I, Böttinger L, Klay D, et al. Long-term expanding human airway organoids for disease modeling. Embo j. 2019;38(4).
4. Boj SF, Hwang CI, Baker LA, Chio, II, Engle DD, Corbo V, et al. Organoid models of human and mouse ductal pancreatic cancer. Cell. 2015;160(1-2):324-38.
5. Lancaster MA, Renner M, Martin CA, Wenzel D, Bicknell LS, Hurles ME, et al. Cerebral organoids model human brain development and microcephaly. Nature. 2013;501(7467):373-9.
6. Wimmer RA, Leopoldi A, Aichinger M, Kerjaschki D, Penninger JM. Generation of blood vessel organoids from human pluripotent stem cells. Nat Protoc. 2019;14(11):3082-100.
7. Wimmer RA, Leopoldi A, Aichinger M, Wick N, Hantusch B, Novatchkova M, et al. Human blood vessel organoids as a model of diabetic vasculopathy. Nature. 2019;565(7740):505-10.
8. Kong D, Ryu JC, Shin N, Lee SE, Kim NG, Kim HY, et al. In Vitro Modeling of Atherosclerosis Using iPSC-Derived Blood Vessel Organoids. Adv Healthc Mater. 2025;14(1):e2400919.
9. Aisenbrey EA, Murphy WL. Synthetic alternatives to Matrigel. Nat Rev Mater. 2020;5(7):539-51.
10. Li K, He Y, Jin X, Jin K, Qian J. Reproducible extracellular matrices for tumor organoid culture: challenges and opportunities. J Transl Med. 2025;23(1):497.
11. Kozlowski MT, Crook CJ, Ku HT. Towards organoid culture without Matrigel. Commun Biol. 2021;4(1):1387.
12. Brassard JA, Lutolf MP. Engineering Stem Cell Self-organization to Build Better Organoids. Cell Stem Cell. 2019;24(6):860-76.

13. Schutgens F, Clevers H. Human Organoids: Tools for Understanding Biology and Treating Diseases. Annu Rev Pathol. 2020;15:211-34.
14. Soto-Gamez A, Gunawan JP, Barazzuol L, Pringle S, Coppes RP. Organoid-based personalized medicine: from tumor outcome prediction to autologous transplantation. Stem Cells. 2024;42(6):499-508.
15. Naderi-Meshkin H, Wahyu Setyaningsih WA, Yacoub A, Carney G, Cornelius VA, Nelson CA, et al. Unveiling impaired vascular function and cellular heterogeneity in diabetic donor-derived vascular organoids. Stem Cells. 2024;42(9):791-808.
16. Ahn Y, An JH, Yang HJ, Lee WJ, Lee SH, Park YH, et al. Blood vessel organoids generated by base editing and harboring single nucleotide variation in Notch3 effectively recapitulate CADASIL-related pathogenesis. Mol Neurobiol. 2024;61(11):9171-83.
17. Gjorevski N, Sachs N, Manfrin A, Giger S, Bragina ME, Ordóñez-Morán P, et al. Designer matrices for intestinal stem cell and organoid culture. Nature. 2016;539(7630):560-4.
18. Giles R, Meijer EM, Maas RGC, van Dijk CGM, Verhaar MC, Cheng C. Animal-free alternatives for Matrigel in human iPSC-derived blood vessel organoid culture. Sci Rep. 2025;15(1):36042.
19. Brandenberg N, Hoehnel S, Kuttler F, Homicsko K, Ceroni C, Ringel T, et al. High-throughput automated organoid culture via stem-cell aggregation in microcavity arrays. Nat Biomed Eng. 2020;4(9):863-74.
20. Quintard C, Tubbs E, Jonsson G, Jiao J, Wang J, Werschler N, et al. A microfluidic platform integrating functional vascularized organoids-on-chip. Nat Commun. 2024;15(1):1452.
21. Tubbs E, Mehanović M, Lopes M, Quintard C, Combe S, Pirlian C, et al. Human assembloid of human blood vessel organoids with pancreatic islets improves insulin secretion over time ex vivo. Cell Rep. 2025;44(10):116378.
22. Heo JH, Kang D, Seo SJ, Jin Y. Engineering the Extracellular Matrix for Organoid Culture. Int J Stem Cells. 2022;15(1):60-9.
23. Moss SP, Bakirci E, Feinberg AW. Engineering the 3D structure of organoids. Stem Cell Reports. 2025;20(1):102379.
24. Nwokoye PN, Abilez OJ. Bioengineering methods for vascularizing organoids. Cell Rep Methods. 2024;4(6):100779.

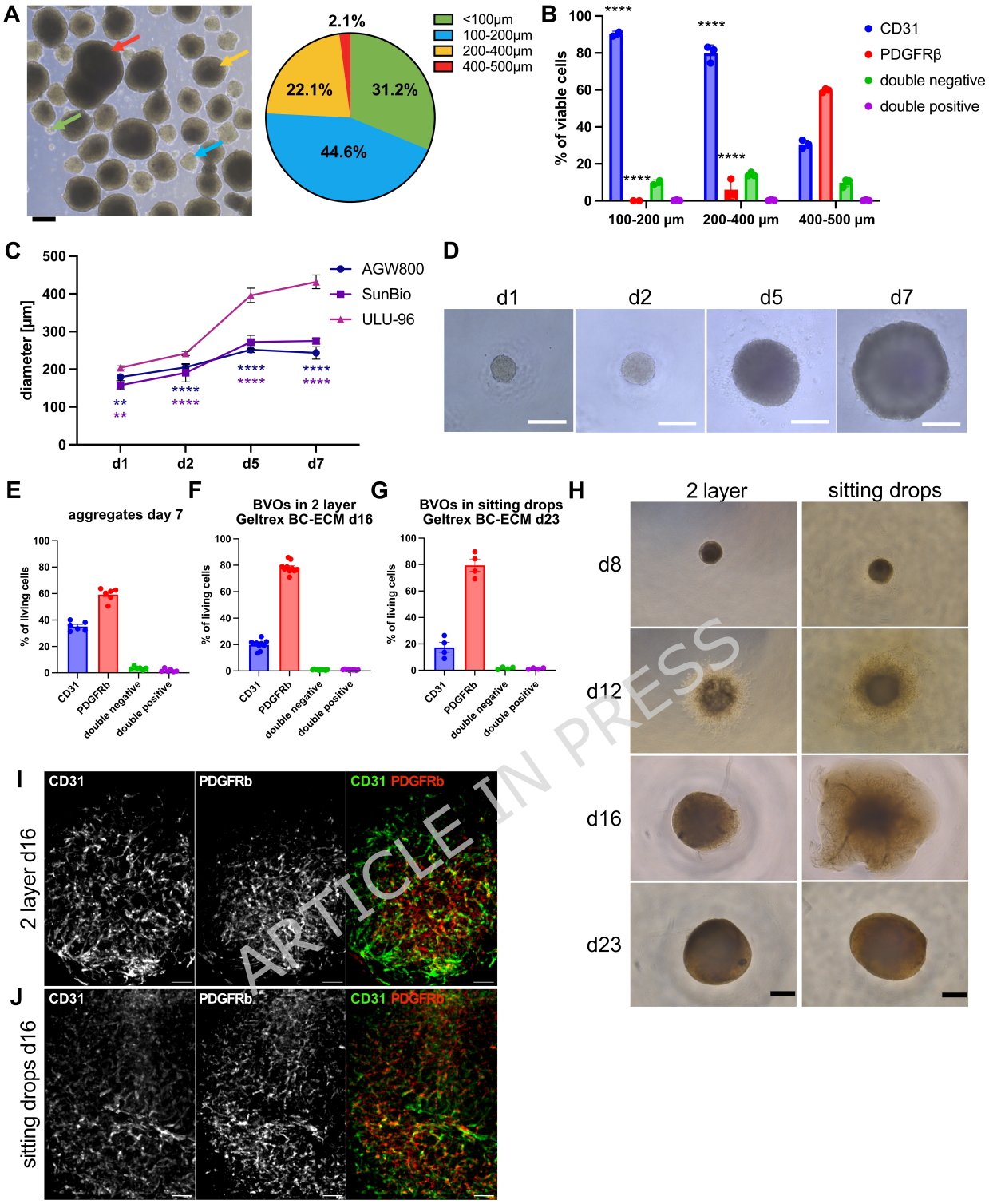

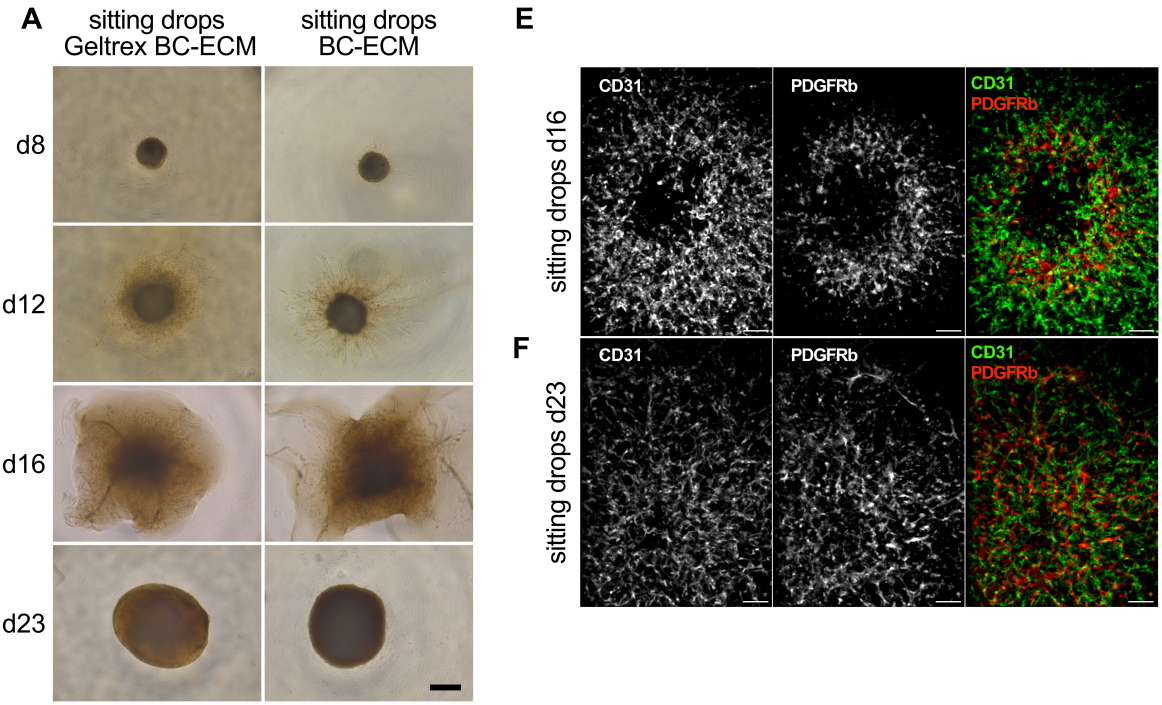

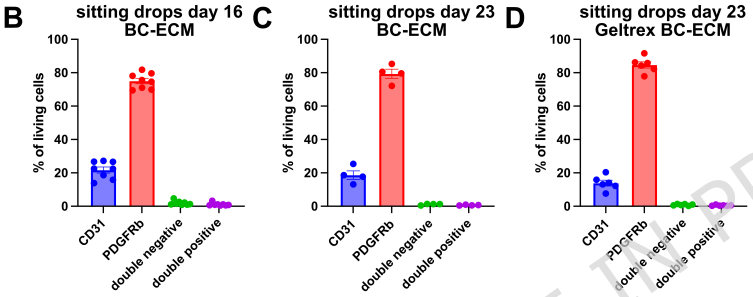

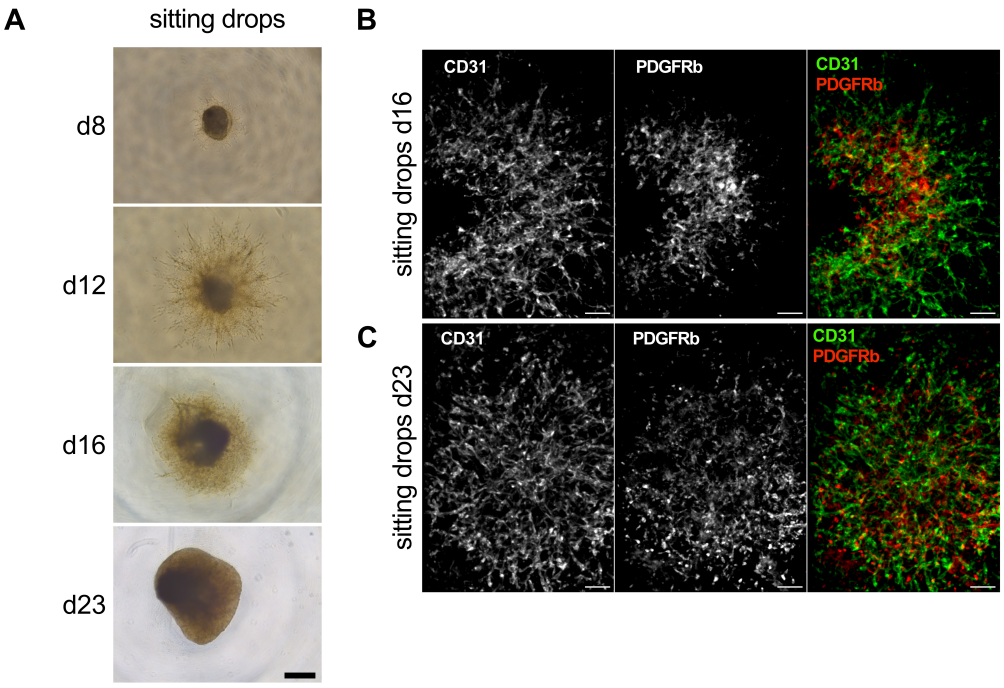

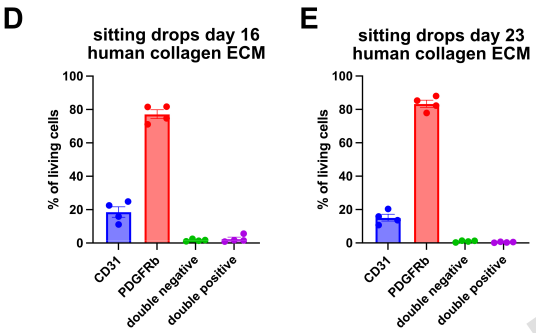

hCD31 **secondary only**